Molecular features underlying *Pseudomonas aeruginosa* persistence in human plasma

Manon Janet-Maitre[1], Stéphane Pont[1*], Frerich Masson[2], Julian Trouillon[1**], Mylène Robert-Genthon[1], Chantal Dumestre-Perrard[3,4], Sylvie Elsen[1], Christine Moriscot[5], Bart Bardoel[2], Suzan Rooijakkers[2], François Cretin[1] and Ina Attrée[1]

[1] University Grenoble Alpes, Institute of Structural Biology, Team Bacterial Pathogenesis and Cellular Responses, 38054 Grenoble, France

[2] Medical Microbiology, University Medical Center Utrecht, Utrecht University, 3584 CX Utrecht, The Netherlands

[3] Laboratory of immunology, Grenoble Alpes University Hospital, cedex 9, 38043 Grenoble, France

[4] University Grenoble Alpes, CNRS, CEA, Institute of Structural Biology (IBS), cedex 9, 38044 Grenoble, France

[5] University Grenoble Alpes, CNRS, CEA, ISBG, F-38000 Grenoble, France

* present address: Laboratory of Pathogen-Host Interactions (LPHI), Université Montpellier, CNRS, UMR5235, 34095 Montpellier cedex 5, France.

** present address: Institute of Molecular Systems Biology, ETH Zurich, Zurich, Switzerland

Abstract

Persistence of bacterial pathogens is a main cause of treatment failure and establishment of chronic bacterial infection. *Pseudomonas aeruginosa*, an opportunistic Gram-negative pathogen is a leading cause of bacteremia with high associated mortality. In a previous study, we found that plasma-sensitive *P. aeruginosa* strains were able to form a persister-like sub-population named evaders. However, the molecular mechanisms underlying emergence and biology of evaders remained unknown. Here, using a gain-of-function genetic screen we examined the molecular determinants of persistence in plasma. In addition to known virulence factors (long O-specific antigens and exopolysaccharides), we found that ATP and biotin availability greatly impact bacterial survival in plasma. Mutants in genes of purine and biotin pathways display higher tolerance and persistence, respectively. Moreover, we identified a novel small protein named SrgA whose expression leads to 100-fold increase in survival in plasma. The analysis of different steps of complement activity and the use of outer-membrane impermeable drug nisin suggest that the mutants impede MAC activity *per se*. Through this work we highlight the multifactorial origin of bacterial resilience to plasma and pave the way to a more comprehensive picture of the complex interplay between *P. aeruginosa* and the complement system in the blood.

48 ## Introduction

49 Human bacterial pathogens employ sophisticated strategies to escape from the
50 immune system and to resist or tolerate antibiotic treatments. Bacterial persistence
51 towards antibiotics is a major obstacle in treatment of life-threatening infections and is
52 frequently associated with the establishment of chronic infections, as it allows the
53 survival of a sub-population that tolerates otherwise lethal antibiotic stress (Fauvart,
54 De Groote, and Michiels 2011; Bartell et al. 2020). Unlike antibiotic resistance,
55 persistence is a non-heritable, fully reversible trait, characterized by a biphasic killing
56 curve with the rapid killing of the bulk population and the survival of a sub-population
57 over a long period of time. Among different factors proposed to lead to antibiotic
58 persistence (Balaban *et al.*, 2019), low intracellular levels of ATP (Shan *et al.*, 2017;
59 Manuse *et al.*, 2021) and production of the "alarmone" signaling molecule guanosine
60 (penta) tetraphosphate, (p)ppGpp (Korch, Henderson and Hill, 2003; Pacios *et al.*,
61 2020) are the most cited. Upon external antibiotic stress, the stochastic or responsive
62 activation of the stringent response leads to accumulation of (p)ppGpp, which in turn
63 activates toxin-antitoxin modules and degradation of the antitoxins through a regulation
64 cascade, leading to inhibition of cell growth (Gaca, Colomer-Winter and Lemos, 2015;
65 Harms, Maisonneuve and Gerdes, 2016). The host immune system also triggers
66 persistence in different bacterial species. Vacuolar acidification after *Salmonella*
67 internalization by macrophages induced persister cell formation and could contribute
68 to the establishment of a bacterial reservoir for infection relapse (Helaine *et al.*, 2014).
69 In a similar manner, human serum triggers the formation of antibiotic persisters as well
70 as so called "viable but non-culturable" forms in *Vibrio vulnificus* (Ayrapetyan *et al.*,
71 2015) and (Putrinš *et al.*, 2015) also highlighted *Escherichia coli* phenotypic
72 heterogeneity leading to serum and antibiotic killing evasion. We previously

demonstrated that a persister-like sub-population of evaders forms when globally sensitive bacteria are incubated in human blood or human plasma. The evaders were documented in several human pathogens including *Pseudomonas aeruginosa* (Pont *et al.*, 2020).

P. aeruginosa is a leading nosocomial pathogen extremely difficult to eradicate due to its high adaptability to different environments, its intrinsic and acquired antibiotic resistance (Moradali, Ghods and Rehm, 2017). The bloodstream infections (BSI) due to *P. aeruginosa* strains hold the highest mortality rate with about 40% (Kang *et al.*, 2003; Vitkauskienė *et al.*, 2010). Interestingly, not all BSI isolates are fully resistant to plasma. Although the complement system (CS) is the major immune component responsible for *P. aeruginosa* killing in human blood and is globally efficient towards sensitive strains, a tiny fraction of the initial bacterial population persists over prolonged incubation in blood and plasma (Pont *et al.*, 2020). Kinetics of *P. aeruginosa* killing by human plasma displays a classical “persister-type” biphasic profile (Balaban *et al.*, 2019), with a rapid elimination of more than 99.9% of the population reaching a plateau at on average 0.1% after a 2h-incubation. We found that out of eleven *P. aeruginosa* isolates tested, three were plasma-resistant, three displayed a tolerant phenotype and five were able to form evaders, suggesting that the evaders may represent a common strategy for *P. aeruginosa* to escape membrane attack complex (MAC)-mediated bactericidal activity in plasma. The plasma evaders differed from antibiotic persisters since a stationary phase population did not give rise to a higher population of evaders as it was shown for antibiotic persisters (Keren *et al.*, 2004) and the mechanisms permitting the evaders to resist the MAC-induced lysis remained unknown. In this work, we refer to resistance, tolerance and persistence as defined in a context of antibiotics in (Balaban *et al.*, 2019). Briefly, resistance is due to the heritable carriage

98 of a resistance factor allowing survival to a higher stress conditions. As opposed to
99 resistance, tolerance is a phenomenon that allows survival of the population to an
100 otherwise lethal stress for a longer period of time without any resistance mechanism.
101 Persistence refers to a heterogeneous bacterial population composed of a rapidly
102 eliminated sensitive population and a tolerant sub-population and is characterized by
103 a biphasic killing curve. We use the term of resilience when including several of these
104 phenomena.

105 In this work we used a genome-wide approach to get first insights into molecular
106 mechanism(s) of *P. aeruginosa* resilience in human plasma. A screen based on
107 transposon-insertion sequencing (Tn-seq) was applied to a recent clinical isolate that
108 showed sensitivity to plasma and displayed 0.01-0.1% of evaders following incubation
109 in plasma for 6h. We hypothesized that the transposon mutants displaying increased
110 percentage of evaders or those with global increased plasma tolerance/resistance
111 could reveal novel determinants of bacterial resilience to plasma and pathogen
112 immune escape. In addition to known *P. aeruginosa* factors involved in plasma
113 resistance, such as lipopolysaccharides (LPS) and exopolysaccharides, we identified
114 an uncharacterized small periplasmic protein whose expression increased
115 complement tolerance up to 100 fold. Moreover, our screen and phenotypic
116 characterization of mutants revealed that the levels of biotin and ATP modulate
117 pathogen sensitivity to MAC-induced lysis.

118 Results

119 Gain-of-function screen in plasma

120 In our previous study we found that the urinary isolate IHMA879472/AZPAE15042
121 (IHMA87) persisted in human blood and plasma. While the global population was

122 sensible to complement killing with 99.9% of the population eliminated within 60
123 minutes, approximately 0.1% evaders survived prolonged incubation in plasma (Pont
124 *et al.*, 2020 and this work). In order to examine molecular determinants leading to
125 persistence in plasma, we searched for hyper-evaders using a genome-wide
126 approach. A transposon library of about 300,000 mutants was constructed using the
127 Himar-1 transposon and insertion mutants with increased levels of survival in plasma
128 were selected using the phenotypic screen schematically presented in Fig. 1A. The
129 transposon library was challenged in native human plasma (output) or heat inactivated
130 plasma (HIP, input) for three hours and recovered. The bacterial survival was
131 determined by colony forming unit (CFU) counts for the whole library before and after
132 the challenge, showing that the global survival increased by about 2-log in the mutant
133 library compared to the parental strain. The screen set-up selects for mutants with
134 global increased survival in plasma. The discrimination between resistant, hyper-
135 evaders and tolerant phenotypes could be appreciated by performing killing curves
136 over a long plasma incubation period.

137 Seven mutants were isolated directly during the screen and their survival was assayed
138 in plasma killing assays. They survived 10 to 200 fold better than the parental strain
139 (Fig. 1B), validating the screen. Among the isolated mutants, two mutants with hyper
140 mucoid phenotypes reflecting alginate overproduction, carried insertions within *mucD*
141 and in the intergenic region upstream of *mucA*, two negative regulators of alginate
142 synthesis (reviewed in Damron and Goldberg, 2012). We also isolated a mutant with
143 the transposon inserted in the intergenic region upstream of *mucE*, a positive regulator
144 of alginate production (Qiu *et al.*, 2007; Yin *et al.*, 2013). The orientation of the
145 transposon suggested that this mutant could overexpress *mucE,* which also led to a
146 mucoid phenotype. The alginate indeed may interfere with the CS by decreasing C3b-

147 dependent opsonization and by interfering with CS activation when acetylated
148 (Pedersen *et al.*, 1990; Pier *et al.*, 2001). A transposon insertion in *ladS*, encoding the
149 histidine kinase positively affecting GacS/GacA-RsmA pathway (Ventre *et al.*, 2006;
150 Broder, Jaeger and Jenal, 2017), resulted in increased mutant survival, by yet
151 unknown effector expression. To note, the bioinformatics analysis of the sequencing
152 data highlighted significant enrichment of transposon insertions in *retS*, a gene
153 encoding for an antagonist to LadS, whose inactivation would lead to increased
154 synthesis of polysaccharides Psl and Pel (Table 1). Indeed, Psl was shown to improve
155 bacterial survival in serum in a mucoid strain (Jones and Wozniak, 2017). The role of
156 Psl in complement resistance might be isolate-dependent, as it was initially shown
157 using the reference strain PAO1, that Psl reduces bacterial opsonization without
158 affecting C9 insertion and survival in serum (Mishra *et al.*, 2012). Moreover, insertion
159 in the promoter of *pprB,* encoding the response regulator acting on type IVb pili/Tad,
160 BapA adhesin and CupE fimbriae expression (Giraud *et al.*, 2011; de Bentzmann *et*
161 *al.*, 2012) also led to increased survival in plasma. As shown, type IV pili contribute to
162 serum resistance and recruitment of host negative complement regulator C4BP in
163 *Vibrio cholerae* and *Neisseria gonorrheae*, respectively (Chiang *et al.*, 1995; Blom *et*
164 *al.*, 2001). Our data suggests that either type IVb pili or CupE-fimbriae could mediate
165 plasma resistance in *P. aeruginosa*. Random picking of colonies did not allow to obtain
166 LPS-related mutants. However, the importance of LPS and more specifically O-specific
167 antigens (OSA) biosyntheses in the interaction with plasma was highlighted by the
168 screen and is in accordance with the literature (Goldberg and Pler, 1996; Priebe *et al.*,
169 2004; Kintz *et al.*, 2008; Osawa *et al.*, 2013). Two isolated clones with increased
170 survival carried the transposon in *bioA* and *bioB*, encoding enzymes of biotin
171 biosynthesis, to our knowledge, not previously linked to resilience to plasma or

172 complement.

173 Analysis of sequencing data was performed for both the insertions in coding regions
174 and insertions in intergenic regions, as the transposon used possesses an outward
175 *tac* promoter, possibly modulating the neighboring gene expression. In both analysis,
176 transposon insertions strongly increasing bacterial survival were associated with four
177 main pathways; *i.e.* biosynthetic pathways of purine and biotin, biosynthesis,
178 production and regulation of the exopolysaccharide alginate (Fig. 1C and Table 1,
179 complete results Table 1S).

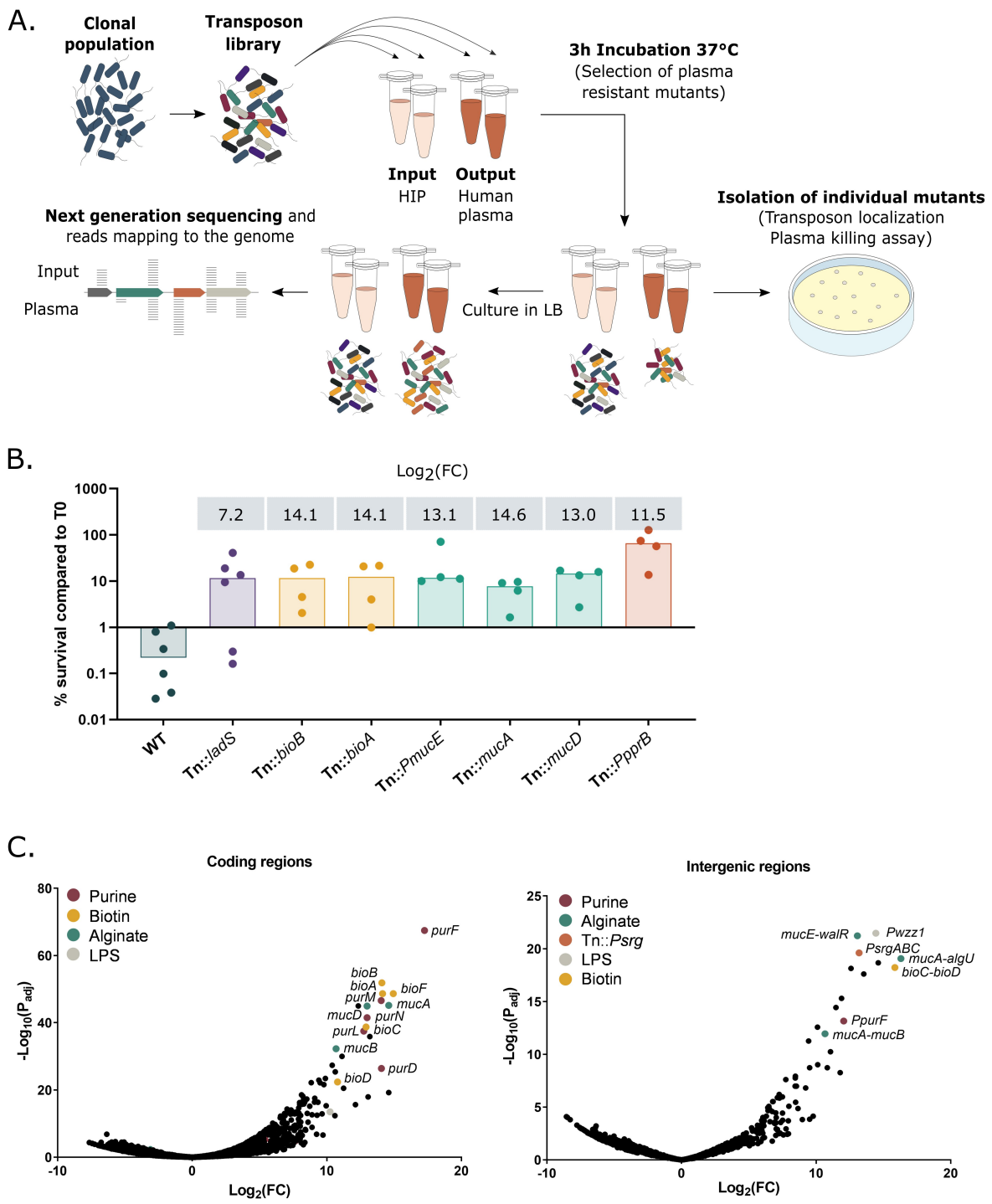

Figure 1. Gain-of-function Tn-seq reveals common as well as novel pathways involved in *P. aeruginosa* survival in plasma. A. Schematic representation of the screen. A transposon mutant library was generated in the plasma-sensitive clinical isolate *P. aeruginosa* IHMA87 and incubated either in human plasma or in HIP (input) for 3h. Aliquots were plated on LB and individual transposon mutants were stored for further analysis. Transposon-insertion sequencing was performed by Illumina-based next generation sequencing. **B.** Survival of isolated transposon mutants in plasma following 3h-incubation. The survival was calculated using CFUs measurements. A

189 log-transformation was performed on the dataset and all mutants were shown
190 significantly different from the wild-type strain (p-value < 0.005). Log_2(Fold-
191 Change(FC)) obtained from the Tn-seq analysis for each gene or intergenic region is
192 indicated above. **C.** Bioinformatics analysis presented as Volcano plots. Insertions in
193 coding regions (left) and intergenic regions (right) were analyzed separately.
194 Significant hits in genes of the same pathway are in the same color.
195
196

IHMA87 ID	PAO1 ID	Name/prediction	Log_2(FC)	P_{adj}
Purine biosynthetic pathway				
IHMA87_01837	*PA3108*	*purF*	17.26	3.64E-68
IHMA87_05343	*PA4855*	*purD*	14.06	3.85E-27
IHMA87_04292	*PA0944*	*purN*	12.99	3.14E-42
IHMA87_04291	*PA0945*	*purM*	14.04	2.51E-47
IHMA87_01191	*PA3763*	*purL*	12.75	3.02E-38
IHMA87_04214	*PA1013*	*purC*	7.67	1.23E-5
IHMA87_02487	*PA2629*	*purB*	5.35	7.23E-4
Biotin biosynthetic pathway				
IHMA87_00400	*PA0420*	*bioA*	14.15	2.29E-49
IHMA87_00477	*PA0501*	*bioF*	14.94	2.29E-49
IHMA87_00476	*PA0500*	*bioB*	14.10	1.39E-52
IHMA87_00479	*PA0503*	*bioC*	12.92	1.90E-39
IHMA87_00480	*PA0504*	*bioD*	10.80	4.23E-23
Alginate biosynthetic/regulation genes				
IHMA87_04494	*PA0762*	*algU*	11.25	3.01E-21
IHMA87_04493	*PA0763*	*mucA*	14.60	6.76E-46
IHMA87_04492	*PA0764*	*mucB*	10.69	5.56E-33
IHMA87_04490	*PA0766*	*mucD*	13.00	1.10E-45
IHMA87_00895	*PA4033*	P_{mucE}	13.07	5.88 E-22
IHMA87_05847	*PA5322*	*algC*	2.66	4.76 E-2
Other top hits				
IHMA87_02894		-	14.60	6.18E-20
IHMA87_02666	*PA2484*	-/transcriptional regulator	13.20	1.33E-36
IHMA87_06317		-	12.34	1.02E-45
IHMA87_01786	*PA3161*	*himD*	12.13	2.38E-16
IHMA87_02554	*PA2573*	-/chemotaxis transducer	11.13	1.02E-30
IHMA87_06033	*PA5490*	*cc4*	10.63	4.10E-26

IHMA87_04274		*slyX*	10.60	4.67E-13
IHMA87_04133	*PA1078*	*flgC*	10.40	4.59E-28
IHMA87_04779	*PA4457*	*kdsD*	10.24	3.15E-14
IHMA87_04779	*PA4457*	-/arabinose-5-phosphate isomerase	10.24	3.15E-14
IHMA87_00896	*PA4032*	*walR*	9.89	3.67E-24
IHMA87_00319	*PA0341*	*lgt*	9.95	5.21E-16
IHMA87_03447	*PA1758*	*pabB*	9.79	2.55E-22
IHMA87_03022	*PA2122*	-/lipid biosynthetic process	9.65	1.27E-13
IHMA87_01755		-	9.51	7.37E-23
IHMA87_04617	*PA4315*	*mvaT*	9.41	1.21E-23
IHMA87_02603		-	9.34	4.46E-17
IHMA87_02570		-	9.28	3.29E-13
IHMA87_05344	*PA4856*	*retS*	9.11	2.94E-18

Table 1. Insertion mutants enriched in plasma compared to HIP in the four main pathways. The genes and pathways showing the most significant (P_{adj}) fold change (Log_2(FC)) in the Tn-seq screen. IHMA87 gene identity (ID) (NCBI accession numbers CP041354 and CP04135), for the chromosome and plasmid sequences respectively (Trouillon *et al.*, 2020) are indicated with PAO1 equivalents where applicable. For each gene, the Log_2(FC) in plasma compared to HIP (input) condition is indicated together with corresponding adjusted *p*-value (P_{adj}), obtained by the DeSeq2 program. The genes are sorted according to their predicted pathway taken from the KEGG database and the *Pseudomonas* genome database (Kanehisa *et al.*, 2008; Winsor *et al.*, 2011).

For several mutants showing >9 Log_2(FC), the transposon was inserted in uncharacterized genes, representing potentially novel key factors of CS evasion (Table 1). Together, those results confirmed the role of LPS, alginates and Psl in resistance to the CS, which validated the Tn-seq approach and pointed toward several novel determinants to explore.

215 **Deficiency in purine and biotin pathways leads to increased persistence**

216 We further focused on hits in genes and intergenic regions of biotin and purine
217 biosynthesis. Mutants with insertions in loci of the entire biotin biosynthesis, the
218 *bioBFHCD* operon and the *bioA* gene, were significantly overrepresented in plasma
219 (Table 1, Fig. 2A), suggesting that the decreased level of biotin leads to better survival
220 in plasma. This finding was surprising, as the biotin pathway was found essential for
221 survival of several pathogens in human serum including *Klebsiella pneumoniae*,
222 *Mycobacterium tuberculosis* (Woong Park *et al.*, 2011; Carfrae *et al.*, 2020; Weber *et*
223 *al.*, 2020). In addition to the mutants isolated from the screen (Tn::*bioA* and Tn::*bioB*),
224 and in order to confirm this result we engineered a *bioB* deletion mutant (Δ*bioB*) and
225 examined its behavior in plasma over a 6h-challenge (Fig. 2B). Compared to the wild-
226 type strain, the fraction of Δ*bioB* that survived in plasma was over 10% compared to
227 about 0.01% of parental strain. Moreover, the survival of IHMA87Δ*bioB* displayed a
228 biphasic killing curve, suggesting that the low level of biotin triggered the persistence
229 in human plasma, in accordance with higher survival of Tn::*bioA* and Tn::*bioB* in
230 plasma (Fig. 1C).

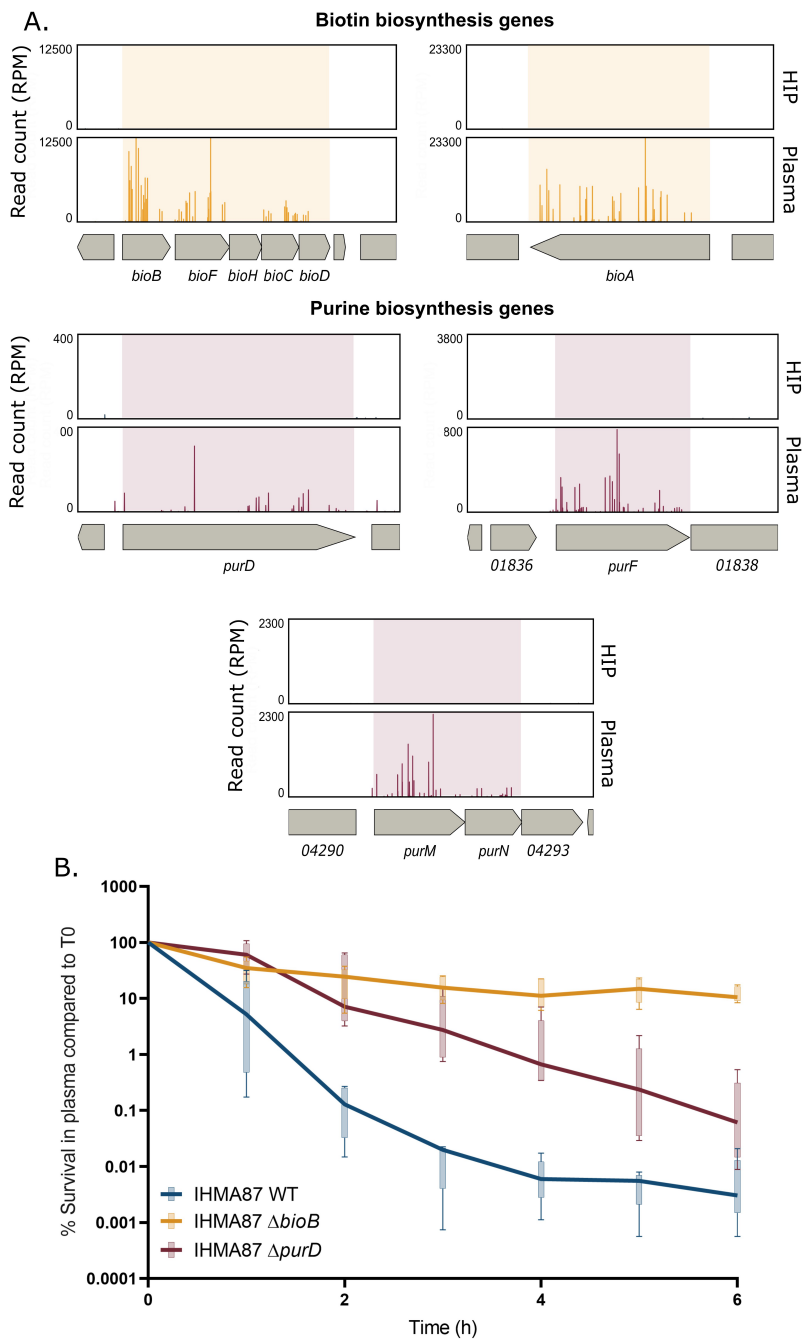

Figure 2. Inactivation of biotin and purine biosynthetic pathways leads to higher survival rates of IHMA87 in plasma. A. Zoom on Tn-seq profiles of *bio* and *pur* genes and operons, showing number of normalized reads in input (HIP) and output (plasma) samples. **B.** Survival kinetics of IHMA87 wild-type strain, Δ*bioB* and Δ*purD* mutants in plasma over 6h incubation measured by CFU counting. Note the biphasic killing curves for the parental strain and Δ*bioB* mutant, indicating increased persistence of Δ*bioB.* The Δ*purD* mutant displayed increased tolerance compared to the parental strain (n=5).

241 *De novo* purine biosynthesis is essential for bacterial nucleotide metabolism together
242 with the pyrimidine pathway and is important for bacterial growth and survival in plasma
243 and serum (Samant *et al.*, 2008; Andersen-Civil *et al.*, 2018; Poulsen *et al.*, 2019; Zhu
244 *et al.*, 2021). Similarly to biotin synthesis, in our model, mutants in the purine
245 biosynthetic pathway clearly displayed increased levels of *P. aeruginosa* survival in
246 plasma (Fig. 2A). Transposon-insertion mutants in three main operons encoding
247 enzymes of purine biogenesis were found overrepresented in the screen. Notably,
248 mutants in *purF*, encoding an amido-phospho-ribosyltransferase were significantly
249 enriched with a Log_2(Fold Change (FC)) of 17.26. To further study the link between
250 purine biosynthesis and increased plasma resistance, we designed a *purD* deletion
251 mutant (Δ*purD*) and investigated its killing kinetics over 6-hours in plasma. In
252 accordance with (Hill *et al.*, 2021) in an antibiotic context, a Δ*purD* mutant displayed
253 a tolerant phenotype in plasma (Fig. 2B). To note, no genes were found to be enriched
254 to the same level in the pyrimidine pathway, suggesting that the specific product of the
255 purine pathway and not global nucleotide metabolism, contributed to increased
256 survival in human plasma.

257

258 **ATP levels influence *P. aeruginosa* tolerance to plasma**

259 Recent studies showed that low ATP levels resulted in increased antibiotic persistence
260 (Shan *et al.*, 2017; Manuse *et al.*, 2021). In the same line, bacteria from the stationary
261 phase of growth have lower levels of intracellular ATP and form a higher proportion of
262 persisters when treated with antibiotics (Conlon *et al.*, 2016). In our hands, growth
263 phase did not contribute significantly to evaders' population suggesting that the initial
264 metabolic status of bacteria had no important role in persistence (Pont *et al.*, 2020).
265 However, because ATP is a final product of the purine pathway (Fig. 3A), we

266 hypothesized that it could also play a role in evaders' formation.
267 To tackle this question, we first measured intracellular ATP levels in Δ*purD* both in rich
268 medium and after incubation in HIP. As expected, Δ*purD* exhibited 5 times lower ATP
269 level than the parental strain (Fig. 3B), and no difference could be observed between
270 HIP and LB. To confirm that the low ATP concentration was indeed responsible for
271 higher resilience to human plasma, we modulated ATP levels by supplementing the
272 plasma with exogenous ATP (Fig. 3C) during plasma killing assay. Indeed, the addition
273 of ATP during the incubation in plasma restored a wild-type-like sensitivity to plasma,
274 further demonstrating the ATP-dependent phenotype of *pur* mutants. To further
275 characterize the *purD* mutant, we investigated potential envelope changes due to the
276 ATP depletion that could account for resistance to MAC killing at the cellular level. We
277 imaged and compared the different strains grown in LB medium or challenged in
278 plasma by transmission electron microscopy (TEM) (Fig. 3E). When grown in LB, the
279 wild-type strain and the Δ*bioB* and Δ*purD* mutants displayed similar size, shape and
280 apparent envelope thickness. However, the Δ*purD* mutant cells occasionally harbor
281 small electron dense granules (Fig. 3E, blue arrow). As expected from its higher
282 sensitivity to plasma, more cell debris was visible on the samples of the wild-type strain
283 incubated in plasma. Interestingly, when Δ*purD* cells were challenged by human
284 plasma, the size and number of the electron dense granules increased (Fig. 3E, red
285 arrows). In wild-type and Δ*bioB* backgrounds, plasma-challenged bacteria displayed
286 small granules, similar to the ones present in the Δ*purD* mutant grown in LB (Fig. 3E,
287 blue arrows). Bibliography mining indicated that these objects may be polyphosphate
288 (Poly-P) storage granules as suggested in (Racki *et al.*, 2017), whose formation is
289 accelerated in stress and starvation conditions. The biotin biosynthesis pathway (Fig.
290 3D) had no apparent link to ATP synthesis. However, as biotin impacts many biological

291 processes, we tested whether a Δ*bioB* mutant could lead to evader formation through
292 a different mechanism. As shown in Figure 3C, biotin but not ATP was able to restore
293 a wild-type-like sensitivity of Δ*bioB* suggesting a distinct molecular mechanism for
294 evader formation in this mutant.

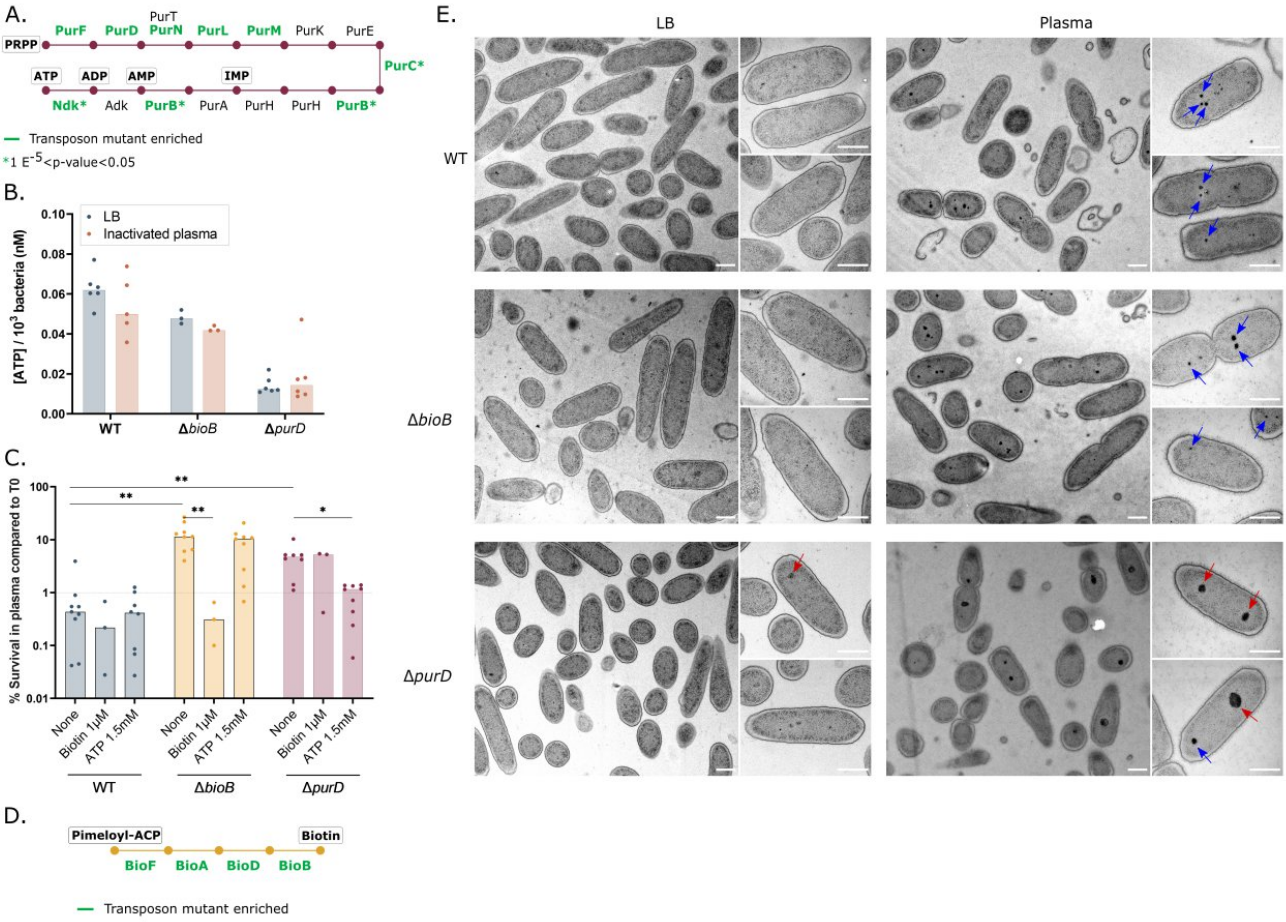

295

296 **Figure 3. ATP and biotin influence bacterial resistance to plasma. A.** Schematic
297 view of purine pathway (adapted from KEGG database (Kanehisa *et al.*, 2008)).
298 Significantly enriched insertions in corresponding genes of the Tn-seq screen are
299 indicated**. B.** Measurement of intra-bacterial ATP levels in LB and after 2h-incubation
300 in HIP normalized to the CFU counts. **C.** Trans-complementation of Δ*bioB* and Δ*purD*
301 phenotype by exogenous biotin or ATP, respectively. Biotin (1 µM) and ATP (1.5 mM)
302 were added at the beginning of the incubation of bacteria in plasma. The survival was
303 estimated by CFU counting. **D.** The biotin biosynthetic pathway. Significantly enriched
304 hits in Tn-seq are highlighted in green. **E.** Transmission electron microscopy images
305 of indicated strains after growth in LB (left) or 1h-incubation in human plasma (right).
306 Red and blue arrow show big- and small-sized granules respectively. Scale bar = 500
307 nm.

308

309

310 **Expression of the three-gene operon *srgABC* leads to better survival in plasma**

311 One mutant isolated during the screen was significantly enriched in plasma with a
312 Log_2(FC) of 13.2 (Fig. 4A). The Sanger sequencing determined the exact transposon
313 insertion within the intergenic region between an uncharacterized predicted three-
314 gene operon *IHMA87_01573–IHMA87_01571* (predicted in PA14 by (Wurtzel *et al.*,
315 2012), corresponding to *PA3369-PA3371* in PAO1) and *panM*
316 (*IHMA87_01574/PA3368*), encoding a shorter version of a probable acetyltransferase
317 (Fig. 4B). The isolated mutant displayed tolerant phenotype over a 6-hour period (Fig.
318 S1) and a 100 fold increase in survival compared to the parental strain after 3h of
319 incubation (Fig. 4C). The position of the transposon and the preliminary RT-qPCR
320 analysis did not allow concluding on the effect of the insertion. In addition, strains
321 carrying deletions either in *panM* or in *IHMA87_01573– IHMA87_01571* in the IHMA87
322 background showed no difference in survival in plasma compared to the wild-type
323 strain (not shown). Therefore, to globally apprehend the transposon-induced changes
324 in the mutant, we determined the transcriptomic profile of the mutant and compared it
325 to the parental strain in LB. The RNA-Seq data showed the overexpression of the
326 predicted *IHMA87_01573-IHMA87_01571* operon, named *srgABC* for serum
327 resistance genes, with about a 20-fold change compared to the parental strain. Thus,
328 the transposon insertion mutant will be referred to as Tn::P_{srg}. All together 90 genes
329 were differentially expressed (|FC|>2, $p_{adj}<1x10^{-10}$) between Tn::P_{srg} and the wild-type
330 strain (Table 2S), including *algU* encoding the alternative sigma factor AlgU and five
331 other alginate genes (*algR* and *mucABCD* operon, Fig. 4D). Consistent with the
332 observed upregulation of *algU*, colonies displayed characteristic mucoïd phenotype
333 on solid medium. The *srg* operon encodes three small putative proteins of 9.9 (SrgA),

334 5.3 (SrgB) and 6.5 (SrgC) kDa. Based on structural predictions, SrgA is a periplasmic
335 or secreted protein presenting the signal peptide cleavage site at position Gly27. Both
336 SrgB and SrgC are predicted membrane proteins with one and two transmembrane
337 alpha-helices for SrgB and SrgC, respectively. The *srg* genes are highly conserved
338 over the 232 complete *P. aeruginosa* genomes available on *Pseudomonas* Genome
339 database (Winsor *et al.*, 2016) with 98-100% amino acid sequence identity.

340 The individual contributions of the *srg* genes in *P. aeruginosa* resilience to plasma
341 were evaluated by testing single, double and triple deletion mutants directly in the
342 Tn::P_{srg} background strain. Plasma killing assay of the mutants showed that SrgA was
343 required and sufficient for increased survival in plasma (Fig. 4C).

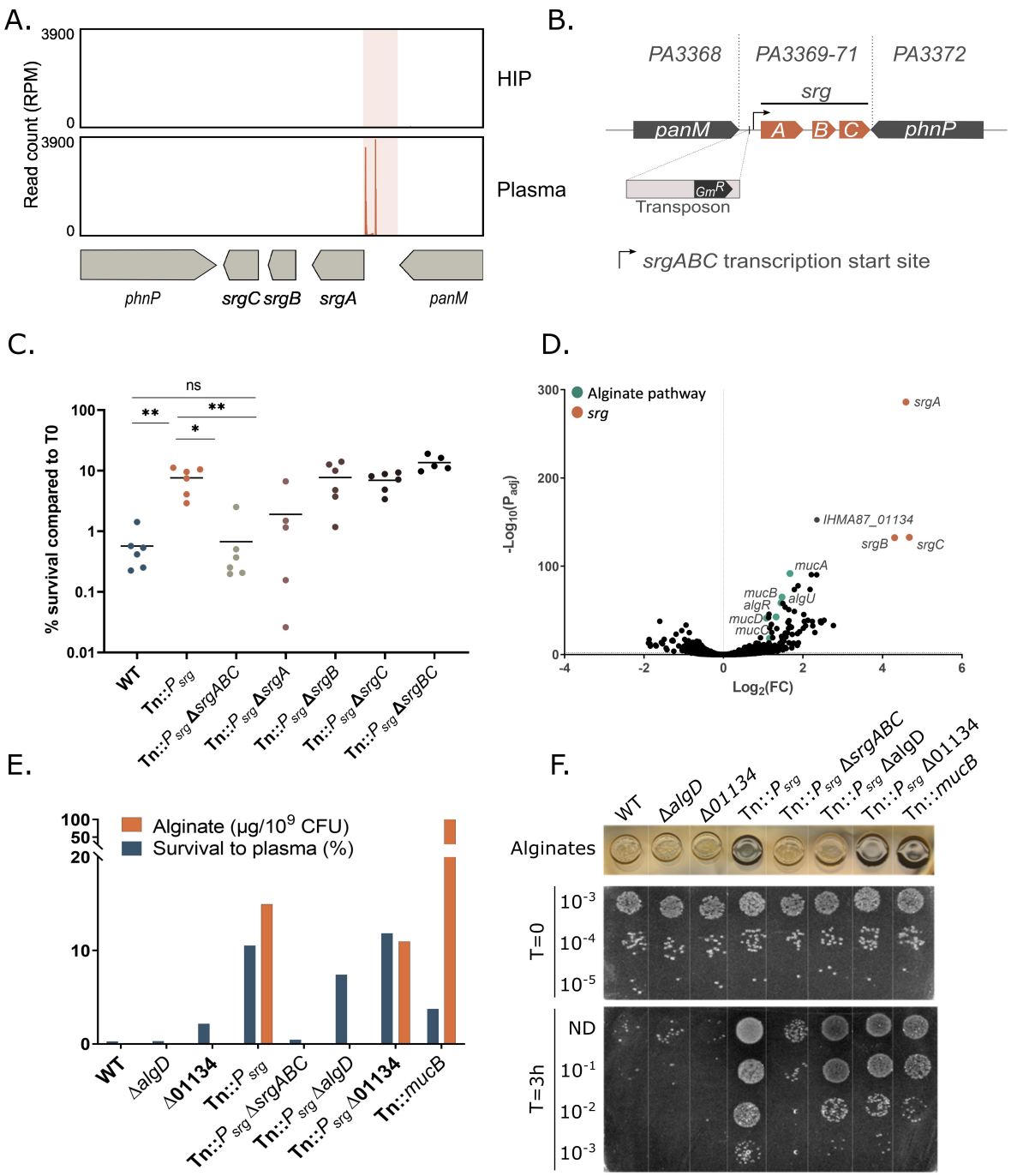

Figure 4. Overexpression of *srgA* leads to a 100-fold increase in survival. A. Zoom into the Tn-seq profiles in the region around the *srg* operon showing number of normalized reads in input (HIP) and output (plasma). **B.** Schematic representation of the predicted *srgABC* operon and position of the transposon in the isolated Tn::P_{srg} mutant as revealed by Sanger sequencing. Corresponding genes from PAO1 are indicated. Note that the transposon is inserted 13 bp upstream of the TSS **C.** Role of individual *srg* genes in the plasma resilience phenotype of the Tn::P_{srg} strain. Note that the deletion of *srgA* restores the sensitivity to plasma. **D.** Differential gene expression between Tn::P_{srg} and the parental IHMA87 strain represented in a volcano plot

354 showing the overexpression of *srgABC* and alginate related genes. RNA was obtained
355 from LB-grown cultures and the whole transcriptomes were determined by RNA-seq
356 pipeline **E-F.** Survival in plasma and alginate production of indicated strains. Alginate
357 synthesis was visualized from colony morphology and quantified by carbazole assay,
358 as described in Materials and methods. Note that alginate overproduction appears as
359 darker bacteria spot (**F**). The data are from one representative experiment, performed
360 in biological triplicates.

361

362 **Contribution of *srgABC* and alginates in tolerance to complement killing**

363 To establish the relationship between the *srg* operon, alginate production and bacterial
364 resilience to complement, we inactivated *algD*, encoding GDP-mannose 6-
365 dehydrogenase, a checkpoint in alginate biosynthesis (Deretic, Gill and Chakrabarty,
366 1987; Berry, DeVault and Chakrabarty, 1989; Wood and Ohman, 2012) both in the
367 parental strain and in Tn::P_{srg}, and investigated relevant phenotypes. In the assay, we
368 included alginate-overproducing mutant Tn::*mucB* isolated during the screen. We also
369 designed a deletion mutant in the gene *IHMA87_01134* (*PA3819*), an uncharacterized
370 gene that was overexpressed (Log_2(FC)=2.35, p_{adj}=2x10^{-153}) in the Tn::P_{srg} strain. For
371 each strain, we established the survival rate by CFU counting, the quantities of
372 alginates using carbazole assay and assessed the colony morphology on plates (Fig.
373 4E-F). The mutant Tn::P_{srg} displayed a 100-fold higher survival in human plasma
374 compared to the parental strain, along with an increased alginate production. Although
375 alginate overproduction can lead to higher resistance to human plasma, as seen for
376 the mutant Tn::*mucB*, the alginates in Tn::P_{srg} did not account significantly for its
377 resistance in plasma. Finally, the deletion of *IHMA87_01134* had no impact neither on
378 alginate production nor on plasma resistance. Overall, these results demonstrate that
379 increased plasma resistance in a *srg* overexpressing mutant is alginate-independent,
380 and that SrgA alone modulates the plasma resistance.

381 **The specificity of mutants toward MAC-induced killing**

382 In order to examine the possible mechanisms leading to increased resistance to
383 bactericidal activity of the MAC in plasma, we set up experiments to survey different
384 steps of the complement cascade. The complement activation of both classical and
385 alternative pathways by bacteria was examined using the measure of residual
386 complement activity toward sensitized sheep or rabbit erythrocytes respectively, as
387 described (Dumestre-Pérard *et al.*, 2008). Plasma incubated with the different mutants
388 exhibited the same level of residual complement capacity to lyse red blood cells as
389 that incubated with the parental strain (Fig. 5A-B), suggesting that complement
390 activation was not altered by the mutants. To investigate whether the mutants are
391 impaired in the formation of C3b and MAC (C5b-9) complexes, we first assessed the
392 deposition of CS components at the bacterial surface by flow cytometry (Fig. 5C-H).
393 As shown on Figure 5C-D, an increase in C3b deposition was observed at 15 min for
394 the the Δ*bioB* mutant. When we exposed bacteria to pooled human serum
395 supplemented with fluorescently labelled C9 (Figure 5E-F), we observed similar
396 deposition of C9, with an apparent increase for the Tn::P_{srg} mutant. Finally, we
397 investigated MAC polymerisation using an anti-C5b-9 antibody and flow cytometry
398 (Fig. G-H). No significant variation in the quantity of the C5b-9 complex was detected
399 between the different mutants, suggesting that globally, the mutants had similar
400 amount of MAC at their surface. To assess the functionality of the inserted MAC pore,
401 we compared serum survival of the different bacteria in the presence of nisin. Normally
402 nisin cannot act on Gram-negative bacteria when they have an intact outer membrane
403 (Heesterbeek *et al.*, 2019). However, MAC-induced damage to the outer-membrane
404 allows the influx of nisin resulting in bacterial killing. As previously shown for plasma,
405 the wild-type displays high sensitivity to killing in serum, with a very efficient bacterial

406 elimination (Fig. 5I). In contrast, survival of all mutants was increased. Interestingly,
407 nisin further killed most of the evaders' population. In a similar manner, the Tn::P_{srg}
408 mutant showed a reduction in numbers in presence of nisin, indicating MAC-induced
409 outer membrane damage. This suggests that outer membrane damage by the MAC
410 itself was not sufficient to kill this mutant or the evaders' population. In contrast, the
411 Δ*bioB* and Δ*purD* strain showed no decreased survival upon nisin addition to the
412 serum. All bacteria could be rescued by addition of C5 inhibitor OmCI, confirming that
413 the killing is complement-driven. Taken together, these data suggest that while the
414 Δ*bioB*, Δ*purD*, and Tn::P_{srg} mutants display increased survival to serum compared to
415 the wild-type, the Tn::P_{srg} mutant interferes at a different stage of MAC-dependent
416 killing than the Δ*bioB* and Δ*purD* mutants.

417

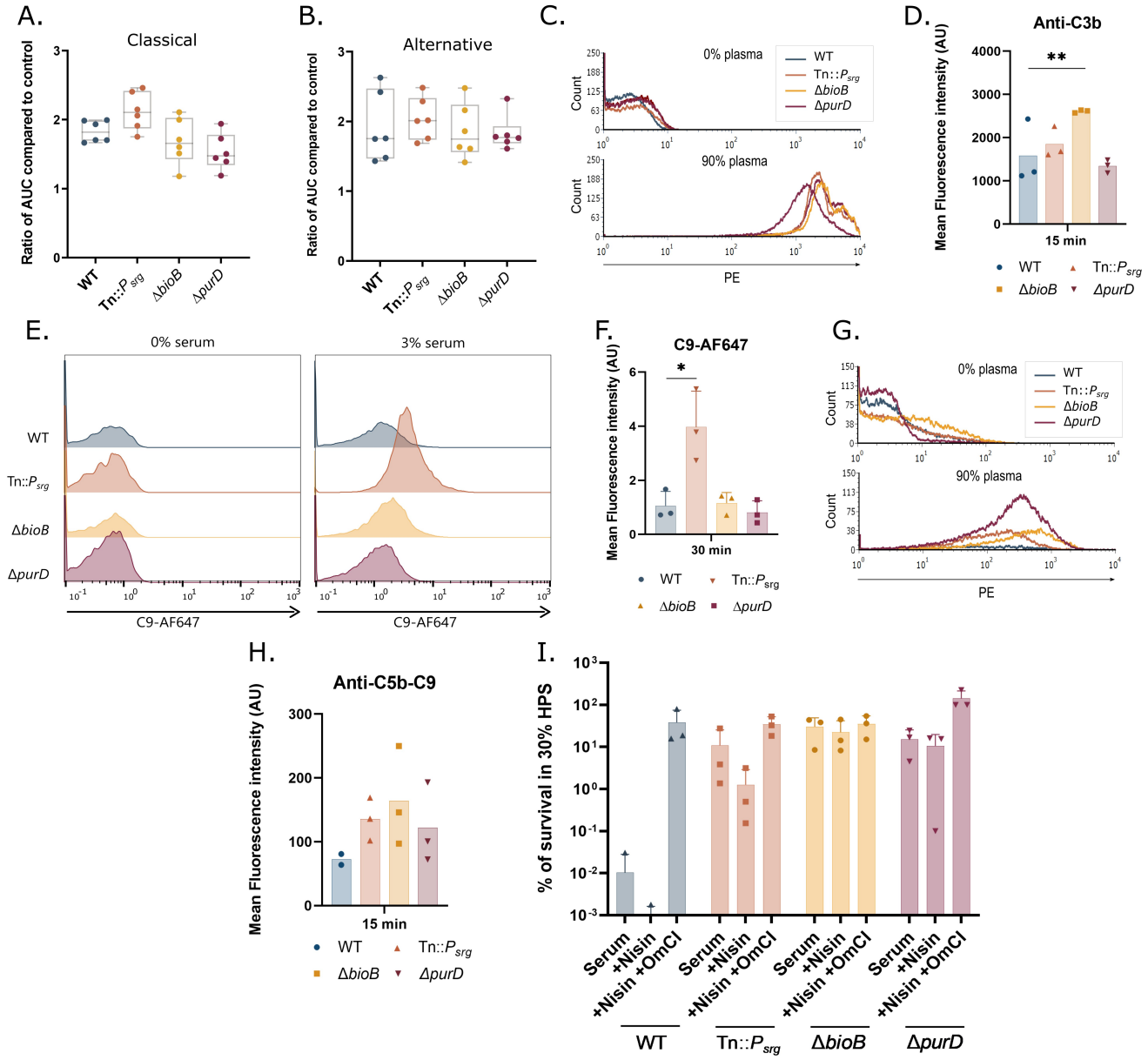

Figure 5. MAC-dependent killing in plasma resilient mutants. Residual complement activity of the classical (**A.**) and alternative (**B.**) complement pathways was measured after bacterial challenge in plasma. n=3. **C.** C3b deposition on bacterial surface after 5 or 15 min of incubation in plasma determined by FACS and **D.** plotted mean fluorescence intensities n=3 p-value < 0.001 when indicated by **. **E.** Bacterial C5b-9 deposition on bacterial surface after 5 or 15min of incubation in plasma determined by FACS and plotted mean fluorescence intensities (**F.**). n=3. **G.** C9-AF647 insertion into bacterial membrane after 30 min in 0% or 3% human pooled serum and **H.** plotted mean fluorescence intensities p-value < 0.05 when indicated by *. **I.** Bacterial survival in human pooled serum, with nisin or in presence of nisin and OmCl complement inhibitor.

431 **Discussion**

432 The variability of *P. aeruginosa* strains concerning their survival in human plasma is
433 high, ranging from fully resistant to sensitive strains. The majority of strains displaying
434 sensitivity at the whole population level form a persistent sub-population with still
435 uncharacterized features (Pont *et al.*, 2020). In this work, we identified ATP, biotin and
436 a small periplasmic protein, named SrgA, as novel molecular determinants of *P.*
437 *aeruginosa* resilience to the CS in human plasma. In accordance with genome-wide
438 screens performed in complement-resistant strains of different pathogens in human
439 serum (Phan *et al.*, 2013; Sanchez-Larrayoz *et al.*, 2017; McCarthy, Stabler and
440 Taylor, 2018; Poulsen *et al.*, 2019; Short *et al.*, 2020), our screen confirmed several
441 previously identified factors, such as LPS, long OSA and exopolysaccharides, as being
442 important for survival of *P. aeruginosa* in human plasma. Also, in agreement with
443 genetic screens that identified bacterial persistence determinants facing antibiotic
444 treatment (Molina-Quiroz *et al.*, 2016; Cameron *et al.*, 2018), we found that persistence
445 in plasma is a multifactorial and probably a stochastic phenomenon. The mutant
446 depleted in intracellular ATP (by a mutation in the purine pathway) showed a higher
447 tolerance profile in plasma and became more MAC-sensitive upon external addition of
448 ATP. In the context of higher tolerance/persistence to antibiotics, it has been proposed
449 that the ATP-depleted conditions would decrease the global protein synthesis and
450 availability of antibiotic targets (Shan *et al.*, 2017). Similarly, the slow growth *per se*,
451 due to any restricted conditions triggers a persistent state (Pontes and Groisman,
452 2019). Although incapable of growing, Δ*bioB* and Δ*purD* mutants were able to survive
453 and persist in HIP for more than 24 hours. Although *in vivo* mutations in the purine and
454 biotin pathways are unlikely to occur, bacteria could use regulatory mechanisms to
455 modulate purine and biotin synthesis and enter in an antibiotic or complement tolerant

456 state. Several reports highlighted the potential of targeting biotin biosynthesis as an
457 alternative antibacterial strategy (Carfrae *et al.*, 2020). Our results showing that the
458 mutants in the biotin biosynthetic pathway are more resistant to microbicidal activity of
459 CS call for more careful assessment of the role of biotin in BSI.

460 The number of plasma evaders following the 2-3h incubation varies between
461 experiments, strains and origin of plasma (Pont *et al.*, 2020); and this work). Therefore,
462 it is possible that the initial incubation in plasma, which is considered as a poor nutritive
463 and stressful milieu for bacteria may stochastically trigger formation of evaders.
464 However, our preliminary results show that pre-incubation of bacteria in HIP does not
465 modify the level of evaders, suggesting that the hostile nutritional environment of HIP
466 is not sufficient to increase the persistence. The adaptation of bacteria to human serum
467 includes upregulation of hundreds of genes, depending on the species. Notably,
468 human blood and serum upregulate quorum sensing genes in plasma-resistant *P.*
469 *aeruginosa* strain PAO1, partly through the global virulence regulator Vfr (Kruczek *et*
470 *al.*, 2014, 2016; Beasley *et al.*, 2020). The serum factors involved in this regulation and
471 downstream effectors are still unknown.

472 In our search for mechanisms underlying escape of here-identified mutants from the
473 complement attack, we found that Tn::P_{srg}, Δ*bioB* and Δ*purD* mutants do not impede
474 complement activation, but probably modulate the function of MAC itself. MAC is a
475 multiprotein pore whose oligomerization occurs by sequential addition of C5b, C6, C7,
476 C8 and finally C9 which forms an oligomeric ring of 18 units inserted into bacterial
477 membranes (Bayly-Jones, Bubeck and Dunstone, 2017). Although the composition of
478 MAC has been known for years, its contribution to bacterial cell death and the way the
479 bacteria die upon MAC insertion is still a debate (Doorduijn, Rooijakkers and
480 Heesterbeek, 2019), and recent work suggested that complement-resistant bacteria

481 can specifically block polymerization of C9 (Doorduijn *et al.*, 2021). SrgA is a protein
482 of 7.1 kDa after predicted signal peptide cleavage, probably localized in the bacterial
483 periplasm and/or exported to the bacterial surface. We can speculate that SrgA directly
484 interferes with MAC assembly. Alternatively, SrgA may act on peptidoglycan or other
485 components of the Gram-negative envelope, which impede MAC function. Our efforts
486 to detect SrgA using protein tags in *P. aeruginosa* were until now unsuccessful, but
487 preliminary visualization of the protein in *E. coli* confirms that the *srgA* gene product is
488 of peptidic nature. However, the nature of *srgB* and *srgC* gene products is completely
489 speculative. The role of ATP in MAC activity is intriguing. No data are available on the
490 requirement of energy in MAC assembly, but we can speculate that it may be required
491 for one of the steps during pore formation. Interestingly, the mutants displayed
492 resistance to an outer-membrane-impermeable polycyclic antibacterial peptide nisin
493 (Heesterbeek *et al.*, 2019), while the majority of the evaders were sensitive. This
494 indicates that, in these mutants, the MAC pore did not allow the nisin incorporation
495 through the permeabilized outer membrane, either due to defective pore insertion or
496 to more resistant inner membranes. On the contrary, the evaders' outer membrane
497 seems to have been damaged by the MAC, suggesting that evaders possess a more
498 resistant envelope or have a quicker ability to repair envelope damage. Further
499 characterization of evaders' biology compared to the bulk population is needed to
500 identify molecular mechanisms triggering the evader state.

501 Taking into account the genetic and phenotypic diversity of *P. aeruginosa* strains
502 (Hilker *et al.*, 2015; Freschi *et al.*, 2018) and their variable levels of survival in human
503 plasma (Pont *et al.*, 2020), we can expect both common and strain-specific
504 determinants that counteract the MAC-dependent killing. Only parallel screens on

505 several representative bacterial strains may deliver the global picture on *P. aeruginosa*
506 plasma and blood resistome/persistome.

507 In an era where bacterial resistance to antibiotics has become the global health
508 concern, any alternative for pathogen elimination could be interesting to explore. The
509 use of a complement system or MAC may be one of those, in combination with
510 classical antibiotics, phages or antibodies that enhance MAC formation (Abd El-Aziz,
511 Elgaml and Ali, 2019; Cruz *et al.*, 2019; Gulati *et al.*, 2019). However, we still have a
512 very limited knowledge on different pathogens strategies to escape the complement.
513 Better understanding of molecular mechanisms involved in pathogen-complement
514 interplay should help designing strategies to fight multi-drug resistant bacteria.
515

516 ## Materials and methods

517 ### Bacterial strains and genetic manipulations

518 Bacterial strains, plasmids and primers are listed in Tables 3S and 4S. *E. coli* and *P.*
519 *aeruginosa* were grown in Lysogeny Broth (LB) at 37°C with shaking (300 rpm). *P.*
520 *aeruginosa* was selected on LB plates containing 25 µg/mL irgasan. Antibiotics
521 concentrations were: 75 µg/mL gentamicin, 75 µg/mL tetracycline and 300 µg/mL
522 carbenicillin for *P. aeruginosa* and 50 µg/mL gentamicin 10 µg/mL tetracycline, 100
523 µg/mL ampicillin for *E. coli*. To create deletion mutants, approximately 500 bp
524 upstream and downstream flanking regions were amplified from genomic DNA by PCR
525 using appropriate primer pairs (sF1/sR1, sF2/sR2). Overlapping fragments were
526 cloned into *Sma*I-digested pEXG2, pEX100T or pEX18Tc by Sequence- and Ligation-
527 Independent Cloning (SLIC, Li and Elledge, 2007). Plasmids were transformed into *E.*
528 *coli* Top10 competent cells and their sequence was verified (Eurofins). Allelic

529 exchange vectors derived from pEXG2, pEX100T or pEX18Tc were introduced into *P.*
530 *aeruginosa* by triparental mating, using pRK600 as a helper plasmid. Merodiploids,
531 resulting from homologous recombinations, were selected on LB agar plate containing
532 irgasan and the appropriate antibiotic. Single merodiploid colonies were streaked on
533 NaCl-free LB plates with 10 % sucrose (w/v), selecting for plasmid loss. Resulting
534 sucrose resistant clones were screened for antibiotic sensitivity and gene deletion by
535 PCR with appropriate primer pairs (F0/R0).

536 **Generation of the IHMA87 transposon library**

537 The IHMA87 transposon mutant library was constructed essentially as previously
538 described (Skurnik *et al.*, 2013; Trouillon *et al.*, 2020). Briefly, IHMA87, grown
539 overnight at 42°C with shaking, was mixed with two *E. coli* strains carrying pRK2013
540 (Figurski and Helinski, 1979) and pBTK24. The conjugation mixtures containing 100
541 µl of each bacterial culture adjusted to optical densities measured at 600 nm (OD_{600})
542 of 1, were centrifuged, washed with LB, deposited onto pre-warmed LB plates and let
543 at 37°C for 5 h. Approximately 100 conjugation mixtures yielded a library of > 300,000
544 mutants. Bacteria were scraped off into liquid LB and aliquots were plated on LB plates
545 containing irgasan (25 µg/ml) and gentamicin (75 µg/ml). Following growth at 37°C,
546 the colonies were collected directly into LB containing 20% glycerol, aliquoted and
547 stored at -80 °C.

548 **Plasma pools preparation**

549 Pools of plasma were prepared from heparinized human blood from healthy donors
550 provided by the French National Blood Institute (EFS, Grenoble, France). Fresh blood
551 was centrifuged for 10 min at 1,000 x g at room temperature. The supernatants of ten
552 different donors were pooled, filtered with a 0.45 µm membrane filter and aliquoted

553 prior to storage at -80 °C until needed. A pool was prepared using the same procedure
554 from citrated blood from 30 healthy donors. Prior to use, plasma pool aliquots were
555 thawed on ice centrifuged 10 min at 10,000 rpm prior to filtration through 0.22 µm
556 membrane. For the heat inactivated plasma (HIP) condition, plasma was thawed and
557 heat inactivated for 30 min at 56°C and centrifuged 10 min at 10,000 rpm prior to
558 filtration through 0.22 µm membrane.

559 **Screen in plasma**

560 A vial containing the IHMA87 mutant library was thawed on ice, transferred into a flask
561 containing 30 mL of LB and grown 16h under agitation at 27°C to limit bacterial growth.
562 The next day, bacterial suspension was diluted to OD_{600nm} ~0.1 and grown at 37°C
563 under agitation. Meanwhile, plasma and HIP were prepared. At an OD_{600nm} ~1, bacteria
564 were harvested and resuspended in PBS supplemented with calcium and magnesium
565 ions (Thermofisher Scientific) before infecting plasma, HIP or LB samples to a
566 concentration of $2.25x10^7$ CFU/mL (90% final plasma concentration). The precise
567 initial CFU count of each experiment was determined by serial dilution. Samples were
568 incubated at 37°C for 3h on a rotating wheel. At the end of the challenge, part of the
569 sample was transferred to LB and grown overnight, part was spread on LB agar plates
570 to isolate individual mutants. Finally, bacterial survival was calculated by CFU counts
571 of each sample. In parallel, the same protocol was performed with the wild-type strain
572 for survival comparison. The next day, vials were taken from the culture and stored for
573 further mutant isolation. About $1x10^9$ bacteria were harvested for each sample and
574 subjected to DNA extraction.

575 **Illumina library construction, sequencing and data analysis**

576 **Genomic DNA.** Bacterial pellets from the screen in plasma with either the HIP samples
577 (Input) or the plasma samples (Output) were used for gDNA preparations. Classical
578 protocol using SDS-NaCl lysis (2% SDS, 0.15M NaCl, 0.1M EDTA pH8, 0.6M Sodium
579 perchlorate) step followed by two successive phenol-chloroform extractions was
580 carried out. The gDNA was precipitated with 100% cold ethanol and diluted in a 200µl
581 TE buffer (10mM Tris-HCl pH8, 1mM EDTA) to final concentration of 50-100 ng/µl.
582 Mechanical DNA shearing was done at 4°C with a QSonica sonicator (Q700) during
583 20 min with 15 second pulses. Fragments were concentrated on columns (Monarch
584 PCR & DNA Cleanup Kit, NEB). The size of generated DNA fragments (150-400 bp)
585 was controlled on 2% agarose gel.

586 **Library construction.** Fragmented gDNA (1 µg) were end-repaired using End-repair
587 module (NEB#E6050) followed by a dA-tailing with Klenow (NEB#6053). Short and
588 Long adaptors (Table 1S) were annealed in 10 mM $MgCl_2$ in thermocycler with a
589 program allowing decrease of 1°C/cycle, from 95°C to 20°C. Ligation of gDNA
590 fragments with annealed adaptors was achieved overnight at 16°C with T4 DNA ligase
591 (NEB#M0202). A size selection was performed on a 2% agarose gel by extracting the
592 bands from 200 to 400 bp (Monarch DNA Gel Extraction Kit, NEB#T1020L).
593 Amplification of purified adaptor-DNA fragments was carried out with Phusion
594 polymerase (NEB#M0530) and specific primers (PCR1 Tn-spe direct and PCR1
595 Adaptor comp.). A second amplification step was performed with a primer carrying a
596 P5 illumina sequence and Indexed-P7 illumina primers (NEB#E7335S). Primer
597 sequences are available on request. After each step, quantification was performed
598 using the Qubit dsDNA HS Assay kit (Q33230). The quality of the libraries was
599 assessed on the Agilent Bioanalyzer 2100 using high-sensitivity DNA chips (Ref

600 #5067-4626). Sequencing was performed on an Illumina NextSeq High (I2BC, Saclay
601 Paris).

602 **Data analysis.** Sequencing reads were trimmed and aligned to the genome of IHMA87
603 using Bowtie2 (Langmead and Salzberg, 2012). Htseq-count (Anders, Pyl and Huber,
604 2015) was then used to obtain read counts per feature. Differential representation of
605 insertion mutants between the plasma and HIP sample was performed using (Love,
606 Huber and Anders, 2014). For the analysis on insertions in intergenic regions, an
607 annotation file was created with intergenic regions attributed to the downstream gene
608 independently of its orientation. The same analysis as above was performed using
609 Htseq-count and DESeq2. Tn-seq was performed in biological duplicates.

610 **Plasma killing assay**

611 Killing assay was performed as described previously (Pont *et al.*, 2020). Unless stated
612 otherwise, bacterial pre-cultures were diluted in LB to OD_{600nm} = 0.1 and grown at 37°C
613 under agitation until OD_{600nm} ~ 1. Bacteria were resuspended into PBS +/+
614 (Thermofisher Scientific) and incubated in plasma to a concentration of $2.25x10^7$
615 CFU/mL (90 % final plasma concentration). The precise initial CFU count of each
616 experiment was determined by serial dilution. Bacterial survival was calculated by CFU
617 counts at the indicated time(s) and compared to the initial count. ATP, biotin and purine
618 were added to the plasma prior to bacterial addition at the indicated concentrations.

619 **Transcriptomics**

620 **RNA extraction.** Bacterial cultures were diluted to an OD_{600nm} of 0.1 and grown at
621 37°C under agitation until they reached an OD_{600nm} of 1. RNA isolation was performed
622 using the hot phenol-chloroform method. Briefly, bacteria were lysed in a hot phenol

623 lysis solution (2 mM EDTA, 1 % SDS, 40mM sodium acetate in acid phenol (Invitrogen
624 #15594-047)). RNA was then isolated by successive steps of phenol-chloroform
625 extraction, followed by one cold chloroform extraction and ethanol precipitations. An
626 additional Turbo DNAse (Invitrogen #AM1907) treatment was performed to remove
627 genomic DNA contamination. Total RNA quantity and quality were assessed using a
628 Agilent Bioanalyzer.

629 **RNA-seq libraries construction.** Following RNA extraction, ribosomal RNAs (rRNAs)
630 depletion was performed using ribominus kit (Invitrogen) according to manufacturer's
631 instructions. Depletion quality was verified on an Agilent Bioanalyzer using RNA pico
632 chips and RNA was concentrated using ethanol precipitation.

633 NEBNext Ultra II directional RNA library prep kit for illumina (NEB) was used to build
634 cDNA libraries for sequencing starting from 50ng of rRNA depleted RNA according to
635 manufacturer's instructions. cDNA libraries quality and concentration were assessed
636 using an Agilent Bioanalyzer High sensitivity DNA chips.

637 **Sequencing and data analysis.** Sequencing was performed by the Institute for
638 Integrative Biology of the Cell (I2BC http://www.i2bc.paris-saclay.fr) high-throughput
639 sequencing facility using an illumina NextSeq500 instrument. More than 12 millions
640 75-bp single-end reads were obtained per sample. Processed reads were mapped
641 onto the IHMA87 genome (available on NCBI CP041354 and CP041355 accession
642 numbers, for the chromosome and plasmid sequences respectively (Trouillon *et al.*,
643 2020)) using Bowtie2 (Langmead and Salzberg, 2012) and the readcount per feature
644 was calculated using Ht-seq count (Anders, Pyl and Huber, 2015). Finally, differential
645 gene expression between the Tn::P_{srg} and the wild-type strains was performed using

646 DESeq2 (Love, Huber and Anders, 2014). RNA-seq experiment was performed on
647 biological duplicates.

648 **Alginate dosage**

649 Equivalent amount of OD_{600nm} adjusted bacterial cultures were spread onto
650 *Pseudomonas* isolation agar (PIA) plates and incubated for 24h at 37°C. Bacterial
651 lawns were flushed with saline solution (0.9% NaCl) and scraped off the plates.
652 Bacteria were pelleted and supernatant was stored in a separated tube. Bacterial pellet
653 was resuspended in LB, incubated on a rotating wheel for 1-2 hours to avoid bacterial
654 aggregates and bacterial titer was calculated by serial dilutions and subsequent CFU
655 counting. The alginate dosage was done as described in Knutson and Jeanes, 1968
656 and May and Chakrabarty, 1994. Briefly, 600µL of ice cold borate working solution
657 (borate stock solution (4 M BO_3^{3-}) diluted to a final concentration of 100 mM in
658 H_2S0_4) were added to 70 µL of the bacteria supernatant, saline solution for blank or
659 commercial sodium alginate solution as standards. Keeping on ice, 20 µL of carbazole
660 solution (0.1% carbazole (Sigma #442506) in 100% ethanol) were added, and samples
661 were incubated at 55°C for 30 min after mixing. The absorbance was measured at 530
662 nm.

663 **Quantitative measurement of intracellular bacterial ATP**

664 For ATP measurement in LB, about 1 x 10^8 bacteria were pelleted and resuspended
665 in PBS. HIP was inoculated with a final concentration of 2.025 x 10^7 bacterial/mL in
666 PBS (90% final HIP concentration). Samples were incubated for 2h at 37°C on a
667 rotating wheel. At the end of the incubation, samples were centrifuged and
668 resuspended in PBS prior to a gentle sonication step using Qsonica sonicator (Q700)
669 for 45 sec with 10% intensity and 5 sec ON-5 sec OFF intervals in order to dissociate

670 the bacterial aggregates. For the two conditions, 10-fold serial dilutions were prepared
671 in 96-well plates and precise bacterial counts were determined by counting CFUs. The
672 concentration of ATP was determined using the BacTiter-Glo kit (Promega, #G8230).
673 Briefly, equal volumes of bacterial suspension and BacTiter-Glo reagent were mixed
674 in white 96-well Lumitrac plates (BioRad #655075) and incubated for 5 min with
675 shaking. An ATP standard curve (0.1 to 100 nM) was established for each experiment.
676 Bioluminescence was measured on a plate reader (Spark, TECAN). ATP
677 concentration was then reported to the CFU counts. Experiments were performed in
678 more than 3 biological replicates.

679 **Residual complement activity**

680 **Sample preparation.** Bacteria grown to $0D_{600nm}$ ~ 1 were resuspended into PBS +/+
681 (Thermofisher Scientific) and incubated in plasma to a concentration of $2.25x10^9$
682 CFU/mL (90% final plasma concentration) or PBS only for the reference. Samples
683 were incubated for 3 hours at 37°C on a rotating wheel to allow complement activation
684 by bacteria. The initial CFU count was determined by serial dilution. At the end of the
685 incubation, samples were centrifuged and supernatant was filtered through 0.22 µm
686 membrane to remove any remaining bacteria. Samples were aliquoted and frozen at
687 -80°C until use. The remaining complement activity in the bacterial/plasma supernatant
688 was measured using a total hemolytic assay for classical and alternative pathways, as
689 described by (Dumestre-Pérard *et al.*, 2008).

690 **Classical complement hemolytic activity.** Briefly, sheep erythrocytes (Orgentec)
691 were sensitized using anti-erythrocytes antibodies (1/40000 - Hemolysin, Orgentec)
692 for 15min at 37°C. Bacterial/plasma supernatant (25 µL) was mixed with 3 mL of
693 sensitized erythrocytes ($4x10^6$ cells/mL) diluted in $DGVB^{2+}$ (2.5% glucose, 0.05%

694 gelatin, 2.5 mM Veronal, 72.5 mM NaCl, 0.15 mM Ca^{2+}, 0.5 mM Mg^{2+}) and lysis kinetic
695 was monitored by OD_{660nm} measurement using a spectrophotometer (safas UVmc2).
696 Area under the curve was measured for each series and reported to the 90% plasma
697 pool control.

698 **Alternative complement hemolytic activity.** Briefly, rabbit erythrocytes (Ecole
699 Nationale Vétérinaire de Toulouse) were washed 3 times using DGVB-Mg-EGTA
700 (2.5% glucose, 0.05% gelatin, 2.5 mM Veronal, 72.5 mM NaCl, 5 mM Mg^{2+}, 3 mM
701 EGTA). Bacterial/plasma supernatant (150 µL) was added to 3 mL of rabbit
702 erythrocytes suspension (diluted in DGVB-Mg-EGTA at 1/250) at 37°C and lysis kinetic
703 was measured similarly to classical complement activity.

704 **C3b and C5b-9 binding assays**

705 Forty millions of bacteria were incubated during 15 min in 90% heparinized plasma
706 pool at 37°C. Incubation was stopped by dilution of bacteria suspension in ten volumes
707 of PBS containing 20 mM of EDTA pH8. C3b binding was detected with PE-conjugated
708 mouse monoclonal anti-C3b/iC3b (5 µg/mL, BioLegend #846103) and C5b-9
709 membrane deposition/insertion was detected with mouse monoclonal anti-C5b-9
710 antibody (8 µg/mL, Abcam #ab66768) next revealed with PE-conjugated goat anti-
711 mouse antibodies (2.5 µg/mL, Abcam #ab97041). Bacteria in 0% plasma were used
712 as negative control. Samples were analyzed in a FACSCalibur instrument (Becton
713 Dickinson) and flow cytometry analysis were performed using the FCSExpress6
714 Software.

715

716

717 **C9 binding**

718 *P. aeruginosa* strains expressing green fluorescent protein (GFP) under the control of
719 the constitutive P_{X2} promoter were grown overnight in LB supplemented with 10 µg/ml
720 tetracycline at 37°C shaking. Bacteria were subcultured 1:30 in LB containing the
721 antibiotic and let grow to a mid-log OD_{600nm} of 0.5 at 37°C with shaking. Bacteria were
722 pelleted by centrifugation, washed, and resuspended to a final OD_{600nm} of 0.05 in RPMI
723 + 0.05% human serum albumin (HSA) for the experiments. Bacteria were then
724 exposed to pooled human serum supplemented with 100 nM C9-AF647 and incubated
725 for 30 minutes at 37°C shaking. For CFU counting, serial bacterial dilutions were made
726 in MilliQ water, spotted on LB plates, and incubated overnight at 37°C. For flow
727 cytometry, bacteria were diluted 10-fold in RPMI-HSA and analyzed in a MACSquant
728 VYB (Miltenyi Biotech) flow cytometer. Bacteria were gated on GFP-expression and
729 subsequently analyzed for AF647 fluorescence. Flow cytometry data was analyzed in
730 FlowJo V.10.

731 **Nisin assay**

732 Bacteria were grown overnight in LB at 37°C shaking, subcultured 1:30 in LB to a mid-
733 log OD_{600nm} of 0.5 at 37°C shaking, pelleted by centrifugation, washed, and
734 resuspended to a final OD_{600nm} of 0.05 in RPMI + 0.05% HSA for the experiments.
735 Bacteria were then exposed to human pooled supplemented with buffer, 3 µg/ml nisin,
736 or 3 µg/ml nisin and 10 µg/ml OmCI, and incubated for 3 hours at 37°C. Serial dilutions
737 were made in MilliQ water, and spotted on LB plates for incubation overnight at 37°C
738 for determination of CFU the next day.

739

740 **Transmission electron microscopy**

741 Bacterial pre-cultures were diluted to an OD_{600nm} of 0.1 in flasks containing 30 mL of
742 LB and incubated at 37°C under agitation. Plasma was then inoculated with bacterial
743 suspension to reach a bacterial concentration of 1.125 $x10^9$ bacteria/mL and incubated
744 on a rotating wheel for 1 hour at 37°C. At the end of the challenge, bacteria were
745 pelleted by centrifugation and resuspended in LB prior to fixation. At the same time,
746 bacteria grown in LB to an OD_{600nm} of 1 were pelleted by centrifugation and
747 resuspended in LB prior to fixation.

748 Sample preparation was treated as described in (Mohamed *et al.*, 2021). Briefly, the
749 cell pellet was spread on the 200-µm side of a 3-mm type A gold plate (Leica
750 Microsystems) covered with the flat side of a 3-mm type B aluminium plate (Leica
751 Microsystems) and vitrified by high-pressure freezing using an HPM100 system (Leica
752 Microsystems). After freezing at -90°C in acetone with 1% OsO4, the samples were
753 slowly warmed to -60°C, stored for 12 hours, then the temperature was increased to -
754 30°C and the samples stored for a further 12 hours before a step at 0°C for 1 hour
755 before being cooled again to -30°C (AFS2; Leica Microsystems). The samples were
756 rinsed 4 times in pure acetone before being infiltrated with progressively increasing
757 concentrations of resin (Epoxy embedding medium, Sigma) in acetone while
758 increasing the temperature to 20°C. Pure resin was added at room temperature. After
759 polymerisation, 70 nm thin sections were obtained using a UC7 ultramicrotome (Leica
760 Microsystems) and collected on 100 mesh copper grids coated with Formvar carbon.
761 The thin sections were post-stained for 5 minutes with 2% uranyl acetate, rinsed with
762 water and incubated for 2 minutes with lead citrate. Samples were observed using a
763 Tecnai G2 Spirit BioTwin microscope (FEI) operating at 120 kV with an Orius SC1000B
764 CCD camera (Gatan).

765 **Bioinformatic analysis and protein conservation**

766 Protein sequence files from all *P. aeruginosa* with a closed assembled genome were
767 retrieved from Pseudomonas genome database and *srg* conservation was investigated
768 using Blast Reciprocal Best Hits program (Cock *et al.*, 2015) computed with a 90%
769 coverage and 50% identity.

770 Signal peptide prediction was perfomed using SignalP website (Almagro Armenteros
771 *et al.*, 2019).

772 **Statistical analysis**

773 Sigmaplot software wasused to perform statistical analysis. Multiple groups
774 comparison was performed using one-way ANOVA or Kruskal-Wallis tests depending
775 on data normality followed by a Student-Newman-Keuls pairwise comparison. Non-
776 normally distributed data were converted to normally-distributed dataset by log_{10}-
777 transformation where indicated. Figures were designed using Graphpad Prism9.

778 **Data availability**

779 The Tn-seq and RNA-seq data generated in this work is available at GEO accession
780 numbers GSExxxxxx and GSExxxxxx respectively.

781 ## Acknowledgments

782 The work was supported by grants from Agence Nationale de la Recherche (ANR-15-
783 CE11-0018-01), the Laboratory of Excellence GRAL, financed within the University
784 Grenoble Alpes graduate school (Écoles Universitaires de Recherche) CBH-EUR-GS
785 (ANR-17-EURE-0003), the Fondation pour la Recherche Médicale (Team FRM 2017,
786 DEQ20170336705) to I.A., the European Union's Horizon 2020 research programs
787 H2020-EU-ITN-EJD (CORVOS #860044 to F.M. and SHMR). The sequencing part

788 has benefited from the facilities and expertise of the high throughput sequencing core
789 facility of I2BC (Centre de Recherche de Gif – http://www.i2bc.paris-saclay.fr/). *P.*
790 *aeruginosa* IHMA87 was obtained from the International Health Management
791 Association, USA. This work used the platforms of the Grenoble Instruct-ERIC center
792 (ISBG; UAR 3518 CNRS-CEA-UGA-EMBL) within the Grenoble Partnership for
793 Structural Biology (PSB), supported by FRISBI (ANR-10-INBS-0005-02) and GRAL,
794 financed within the University Grenoble Alpes graduate school (Ecoles Universitaires
795 de Recherche) CBH-EUR-GS (ANR-17-EURE-0003). M. JM received a Ph.D.
796 fellowship from the French Ministry of Education and Research. The IBS Electron
797 Microscope facility is supported by the Auvergne Rhône-Alpes Region, the Fonds
798 Feder, the Fondation pour la Recherche Médicale and GIS-IBiSA. The authors thank
799 Benoît Gallet and Emily Rey for their help for TEM and mutant analyses, respectively.
800 M.JM thanks Tweeter followers for indicating literature on PolyP granules.

801

802 **Bibliography**

803 Abd El-Aziz, A.M., Elgaml, A. and Ali, Y.M. (2019) 'Bacteriophage Therapy Increases
804 Complement-Mediated Lysis of Bacteria and Enhances Bacterial Clearance After
805 Acute Lung Infection With Multidrug-Resistant Pseudomonas aeruginosa', *The Journal*
806 *of Infectious Diseases*, 219(9), pp. 1439–1447. doi:10.1093/infdis/jiy678.

807 Almagro Armenteros, J.J. *et al.* (2019) 'SignalP 5.0 improves signal peptide predictions
808 using deep neural networks', *Nature Biotechnology*, 37(4), pp. 420–423.
809 doi:10.1038/s41587-019-0036-z.

810 Anders, S., Pyl, P.T. and Huber, W. (2015) 'HTSeq—a Python framework to work with
811 high-throughput sequencing data', *Bioinformatics*, 31(2), pp. 166–169.
812 doi:10.1093/bioinformatics/btu638.

813 Andersen-Civil, A.I.S. *et al.* (2018) 'The impact of inactivation of the purine biosynthesis
814 genes, purN and purT, on growth and virulence in uropathogenic E. coli', *Molecular*
815 *Biology Reports*, 45(6), pp. 2707–2716. doi:10.1007/s11033-018-4441-z.

816 Ayrapetyan, M. *et al.* (2015) 'Viable but Nonculturable and Persister Cells Coexist
817 Stochastically and Are Induced by Human Serum', *Infection and Immunity*, 83(11), pp.
818 4194–4203. doi:10.1128/IAI.00404-15.

819 Balaban, N.Q. *et al.* (2019) 'Definitions and guidelines for research on antibiotic
820 persistence (vol 17, pg 441, 2019)', *Nature Reviews Microbiology*, 17(7), pp. 460–460.
821 doi:10.1038/s41579-019-0207-4.

822 Bartell, J.A. *et al.* (2020) 'Bacterial persisters in long-term infection: Emergence and
823 fitness in a complex host environment', *PLoS pathogens*, 16(12), p. e1009112.
824 doi:10.1371/journal.ppat.1009112.

825 Bayly-Jones, C., Bubeck, D. and Dunstone, M.A. (2017) 'The mystery behind
826 membrane insertion: a review of the complement membrane attack complex',
827 *Philosophical Transactions of the Royal Society B: Biological Sciences*, 372(1726), p.
828 20160221. doi:10.1098/rstb.2016.0221.

829 Beasley, K.L. *et al.* (2020) 'During bacteremia, Pseudomonas aeruginosa PAO1
830 adapts by altering the expression of numerous virulence genes including those
831 involved in quorum sensing', *PLOS ONE*. Edited by R.M. Roop, 15(10), p. e0240351.
832 doi:10.1371/journal.pone.0240351.

833 de Bentzmann, S. *et al.* (2012) 'Unique Biofilm Signature, Drug Susceptibility and
834 Decreased Virulence in Drosophila through the Pseudomonas aeruginosa Two-
835 Component System PprAB', *PLoS Pathogens*. Edited by D.S. Schneider, 8(11), p.
836 e1003052. doi:10.1371/journal.ppat.1003052.

837 Berry, A., DeVault, J.D. and Chakrabarty, A.M. (1989) 'High osmolarity is a signal for
838 enhanced algD transcription in mucoid and nonmucoid Pseudomonas aeruginosa
839 strains', *Journal of Bacteriology*, 171(5), pp. 2312–2317. doi:10.1128/jb.171.5.2312-
840 2317.1989.

841 Blom, A.M. *et al.* (2001) 'A Novel Interaction Between Type IV Pili of Neisseria
842 gonorrhoeae and the Human Complement Regulator C4b-Binding Protein', *The*
843 *Journal of Immunology*, 166(11), pp. 6764–6770. doi:10.4049/jimmunol.166.11.6764.

844 Broder, U.N., Jaeger, T. and Jenal, U. (2017) 'LadS is a calcium-responsive kinase
845 that induces acute-to-chronic virulence switch in Pseudomonas aeruginosa', *Nature*
846 *Microbiology*, 2(1), p. 16184. doi:10.1038/nmicrobiol.2016.184.

847 Cameron, D.R. *et al.* (2018) 'A Genetic Determinant of Persister Cell Formation in
848 Bacterial Pathogens', *Journal of Bacteriology*. Edited by G. O'Toole, 200(17).
849 doi:10.1128/JB.00303-18.

850 Carfrae, L.A. *et al.* (2020) 'Mimicking the human environment in mice reveals that
851 inhibiting biotin biosynthesis is effective against antibiotic-resistant pathogens', *Nature*
852 *Microbiology*, 5(1), pp. 93–101. doi:10.1038/s41564-019-0595-2.

853 Chiang, S.L. *et al.* (1995) 'Single amino acid substitutions in the N-terminus of Vibrio
854 cholerae TcpA affect colonization, autoagglutination, and serum resistance', *Molecular*
855 *Microbiology*, 17(6), pp. 1133–1142. doi:10.1111/j.1365-2958.1995.mmi_17061133.x.

856 Cock, P.J.A. *et al.* (2015) 'NCBI BLAST+ integrated into Galaxy', *GigaScience*, 4(1),
857 pp. s13742-015-0080–7. doi:10.1186/s13742-015-0080-7.

858 Conlon, B.P. *et al.* (2016) 'Persister formation in Staphylococcus aureus is associated
859 with ATP depletion', *Nature Microbiology*, 1(5), pp. 1–7.
860 doi:10.1038/nmicrobiol.2016.51.

861 Cruz, J.W. *et al.* (2019) 'A novel bispecific antibody platform to direct complement
862 activity for efficient lysis of target cells', *Scientific Reports*, 9(1), p. 12031.
863 doi:10.1038/s41598-019-48461-1.

864 Damron, F.H. and Goldberg, J.B. (2012) 'Proteolytic regulation of alginate
865 overproduction in Pseudomonas aeruginosa: Proteolytic regulation of alginate',
866 *Molecular Microbiology*, 84(4), pp. 595–607. doi:10.1111/j.1365-2958.2012.08049.x.

867 Deretic, V., Gill, J.F. and Chakrabarty, A.M. (1987) '*Pseudomonas aeruginosa*
868 infection in cystic fibrosis: nucleotide sequence and transcriptional regulation of the
869 *algD* gene', *Nucleic Acids Research*, 15(11), pp. 4567–4581.
870 doi:10.1093/nar/15.11.4567.

871 Doorduijn, D.J. *et al.* (2021) 'Polymerization of C9 enhances bacterial cell envelope
872 damage and killing by membrane attack complex pores', *PLOS Pathogens*, 17(11), p.
873 e1010051. doi:10.1371/journal.ppat.1010051.

874 Doorduijn, D.J., Rooijakkers, S.H.M. and Heesterbeek, D.A.C. (2019) 'How the
875 Membrane Attack Complex Damages the Bacterial Cell Envelope and Kills Gram-
876 Negative Bacteria', *BioEssays*, 41(10), p. 1900074. doi:10.1002/bies.201900074.

877 Dumestre-Pérard, C. *et al.* (2008) '*Aspergillus* Conidia Activate the Complement by
878 the Mannan-Binding Lectin C2 Bypass Mechanism', *The Journal of Immunology*,
879 181(10), pp. 7100–7105. doi:10.4049/jimmunol.181.10.7100.

880 Fauvart, M., De Groote, V.N. and Michiels, J. (2011) 'Role of persister cells in chronic
881 infections: clinical relevance and perspectives on anti-persister therapies', *Journal of*
882 *Medical Microbiology*, 60(Pt 6), pp. 699–709. doi:10.1099/jmm.0.030932-0.

883 Figurski, D.H. and Helinski, D.R. (1979) 'Replication of an origin-containing derivative
884 of plasmid RK2 dependent on a plasmid function provided in trans', *Proceedings of*
885 *the National Academy of Sciences of the United States of America*, 76(4), pp.
886 1648–1652.

887 Freschi, L. *et al.* (2018) 'Genomic characterisation of an international Pseudomonas
888 aeruginosa reference panel indicates that the two major groups draw upon distinct
889 mobile gene pools', *FEMS Microbiology Letters*, 365(14). doi:10.1093/femsle/fny120.

890 Gaca, A.O., Colomer-Winter, C. and Lemos, J.A. (2015) 'Many Means to a Common
891 End: the Intricacies of (p)ppGpp Metabolism and Its Control of Bacterial Homeostasis',
892 *Journal of Bacteriology*, 197(7), pp. 1146–1156. doi:10.1128/JB.02577-14.

893 Giraud, C. *et al.* (2011) 'The PprA-PprB two-component system activates CupE, the
894 first non-archetypal Pseudomonas aeruginosa chaperone-usher pathway system

895 assembling fimbriae: P. aeruginosa CupE fimbriae', *Environmental Microbiology*,
896 13(3), pp. 666–683. doi:10.1111/j.1462-2920.2010.02372.x.

897 Goldberg, J.B. and Pler, G.B. (1996) 'Pseudomonas aeruginosa lipopolysaccharides
898 and pathogenesis', *Trends in Microbiology*, 4(12), pp. 490–494. doi:10.1016/s0966-
899 842x(97)82911-3.

900 Gulati, S. *et al.* (2019) 'Complement alone drives efficacy of a chimeric antigonococcal
901 monoclonal antibody', *PLOS Biology*. Edited by M.K. Waldor, 17(6), p. e3000323.
902 doi:10.1371/journal.pbio.3000323.

903 Harms, A., Maisonneuve, E. and Gerdes, K. (2016) 'Mechanisms of bacterial
904 persistence during stress and antibiotic exposure', *Science*, 354(6318).
905 doi:10.1126/science.aaf4268.

906 Heesterbeek, D. a. C. *et al.* (2019) 'Complement-dependent outer membrane
907 perturbation sensitizes Gram-negative bacteria to Gram-positive specific antibiotics',
908 *Scientific Reports*, 9(1), p. 3074. doi:10.1038/s41598-019-38577-9.

909 Helaine, S. *et al.* (2014) 'Internalization of Salmonella by macrophages induces
910 formation of nonreplicating persisters', *Science (New York, N.Y.)*, 343(6167), pp.
911 204–208. doi:10.1126/science.1244705.

912 Hilker, R. *et al.* (2015) 'Interclonal gradient of virulence in the Pseudomonas
913 aeruginosa pangenome from disease and environment', *Environmental Microbiology*,
914 17(1), pp. 29–46. doi:10.1111/1462-2920.12606.

915 Hill, P.W.S. *et al.* (2021) 'The vulnerable versatility of Salmonella antibiotic persisters
916 during infection', *Cell Host & Microbe* [Preprint]. doi:10.1016/j.chom.2021.10.002.

917 Jones, C.J. and Wozniak, D.J. (2017) 'Psl Produced by Mucoid Pseudomonas
918 aeruginosa Contributes to the Establishment of Biofilms and Immune Evasion', *mBio*.
919 Edited by J.B. Goldberg, 8(3), pp. e00864-17, /mbio/8/3/e00864-17.atom.
920 doi:10.1128/mBio.00864-17.

921 Kanehisa, M. *et al.* (2008) 'KEGG for linking genomes to life and the environment',
922 *Nucleic Acids Research*, 36(suppl_1), pp. D480–D484. doi:10.1093/nar/gkm882.

923 Kang, C.-I. *et al.* (2003) 'Pseudomonas aeruginosa Bacteremia: Risk Factors for
924 Mortality and Influence of Delayed Receipt of Effective Antimicrobial Therapy on
925 Clinical Outcome', *Clinical Infectious Diseases*, 37(6), pp. 745–751.
926 doi:10.1086/377200.

927 Keren, I. *et al.* (2004) 'Persister cells and tolerance to antimicrobials', *FEMS*
928 *Microbiology Letters*, 230(1), pp. 13–18. doi:10.1016/S0378-1097(03)00856-5.

929 Kintz, E. *et al.* (2008) 'Lipopolysaccharide O-Antigen Chain Length Regulation in
930 Pseudomonas aeruginosa Serogroup O11 Strain PA103', *Journal of Bacteriology*,
931 190(8), pp. 2709–2716. doi:10.1128/JB.01646-07.

932 Knutson, C.A. and Jeanes, A. (1968) 'A new modification of the carbazole analysis:
933 application to heteropolysaccharides', *Anal Biochem*, 24(3), pp. 470–81.
934 doi:10.1016/0003-2697(68)90154-1.

935 Korch, S.B., Henderson, T.A. and Hill, T.M. (2003) 'Characterization of the hipA7 allele
936 of Escherichia coli and evidence that high persistence is governed by (p)ppGpp
937 synthesis', *Molecular Microbiology*, 50(4), pp. 1199–1213. doi:10.1046/j.1365-
938 2958.2003.03779.x.

939 Kruczek, C. *et al.* (2014) 'Serum influences the expression of Pseudomonas
940 aeruginosa quorum-sensing genes and QS-controlled virulence genes during early
941 and late stages of growth', *MicrobiologyOpen*, 3(1), pp. 64–79. doi:10.1002/mbo3.147.

942 Kruczek, C. *et al.* (2016) 'Major Transcriptome Changes Accompany the Growth of
943 Pseudomonas aeruginosa in Blood from Patients with Severe Thermal Injuries', *PLOS*
944 *ONE*. Edited by R.M. Roop II, 11(3), p. e0149229. doi:10.1371/journal.pone.0149229.

945 Langmead, B. and Salzberg, S.L. (2012) 'Fast gapped-read alignment with Bowtie 2',
946 *Nature Methods*, 9(4), pp. 357–359. doi:10.1038/nmeth.1923.

947 Li, M.Z. and Elledge, S.J. (2007) 'Harnessing homologous recombination in vitro to
948 generate recombinant DNA via SLIC', *Nature Methods*, 4(3), pp. 251–256.
949 doi:10.1038/nmeth1010.

950 Love, M.I., Huber, W. and Anders, S. (2014) 'Moderated estimation of fold change and
951 dispersion for RNA-seq data with DESeq2', *Genome Biology*, 15(12), p. 550.
952 doi:10.1186/s13059-014-0550-8.

953 Manuse, S. *et al.* (2021) 'Bacterial persisters are a stochastically formed subpopulation
954 of low-energy cells', *PLOS Biology*. Edited by T. Bollenbach, 19(4), p. e3001194.
955 doi:10.1371/journal.pbio.3001194.

956 May, T.B. and Chakrabarty, A.M. (1994) '[22] Isolation and assay of Pseudomonas
957 aeruginosa alginate', in *Methods in Enzymology*. Academic Press (Bacterial
958 Pathogenesis Part A: Identification and Regulation of Virulence Factors), pp. 295–304.
959 doi:10.1016/0076-6879(94)35148-1.

960 McCarthy, A.J., Stabler, R.A. and Taylor, P.W. (2018) 'Genome-Wide Identification by
961 Transposon Insertion Sequencing of Escherichia coli K1 Genes Essential for In Vitro
962 Growth, Gastrointestinal Colonizing Capacity, and Survival in Serum', *Journal of*
963 *Bacteriology*, 200(7). doi:10.1128/JB.00698-17.

964 Mishra, M. *et al.* (2012) 'Pseudomonas aeruginosa Psl polysaccharide reduces
965 neutrophil phagocytosis and the oxidative response by limiting complement-mediated
966 opsonization', *Cellular Microbiology*, 14(1), pp. 95–106. doi:10.1111/j.1462-
967 5822.2011.01704.x.

968 Mohamed, A.M.T. *et al.* (2021) 'Chromosome Segregation and Peptidoglycan
969 Remodeling Are Coordinated at a Highly Stabilized Septal Pore to Maintain Bacterial
970 Spore Development', *Developmental Cell*, 56(1), pp. 36-51.e5.
971 doi:10.1016/j.devcel.2020.12.006.

Molina-Quiroz, R.C. *et al.* (2016) 'Transposon-Sequencing Analysis Unveils Novel Genes Involved in the Generation of Persister Cells in Uropathogenic Escherichia coli', *Antimicrobial Agents and Chemotherapy*, 60(11), pp. 6907–6910. doi:10.1128/AAC.01617-16.

Moradali, M.F., Ghods, S. and Rehm, B.H.A. (2017) 'Pseudomonas aeruginosa Lifestyle: A Paradigm for Adaptation, Survival, and Persistence', *Frontiers in Cellular and Infection Microbiology*, 7, p. 39. doi:10.3389/fcimb.2017.00039.

Osawa, K. *et al.* (2013) 'Modulation of O-antigen chain length by the wzz gene in Escherichia coli O157 influences its sensitivities to serum complement', *Microbiol Immunol*, 57(9), pp. 616–23. doi:10.1111/1348-0421.12084.

Pacios, O. *et al.* (2020) '(p)ppGpp and Its Role in Bacterial Persistence: New Challenges', *Antimicrobial Agents and Chemotherapy*, 64(10), pp. e01283-20. doi:10.1128/AAC.01283-20.

Pedersen, S.S. *et al.* (1990) 'Pseudomonas aeruginosa alginate in cystic fibrosis sputum and the inflammatory response', *Infection and Immunity*, 58(10), pp. 3363–3368. doi:10.1128/iai.58.10.3363-3368.1990.

Phan, M.-D. *et al.* (2013) 'The serum resistome of a globally disseminated multidrug resistant uropathogenic Escherichia coli clone', *PLoS genetics*, 9(10), p. e1003834. doi:10.1371/journal.pgen.1003834.

Pier, G.B. *et al.* (2001) 'Role of alginate O acetylation in resistance of mucoid Pseudomonas aeruginosa to opsonic phagocytosis', *Infection and Immunity*, 69(3), pp. 1895–1901. doi:10.1128/IAI.69.3.1895-1901.2001.

Pont, S. *et al.* (2020) 'Bacterial behavior in human blood reveals complement evaders with some persister-like features', *PLoS Pathog*, 16(12), p. e1008893. doi:10.1371/journal.ppat.1008893.

Pontes, M.H. and Groisman, E.A. (2019) 'Slow growth determines nonheritable antibiotic resistance in Salmonella enterica', *Sci Signal*, 12(592). doi:10.1126/scisignal.aax3938.

Poulsen, B.E. *et al.* (2019) 'Defining the core essential genome of Pseudomonas aeruginosa', *Proceedings of the National Academy of Sciences*, 116(20), pp. 10072–10080. doi:10.1073/pnas.1900570116.

Priebe, G.P. *et al.* (2004) 'The galU Gene of Pseudomonas aeruginosa is required for corneal infection and efficient systemic spread following pneumonia but not for infection confined to the lung', *Infection and Immunity*, 72(7), pp. 4224–4232. doi:10.1128/IAI.72.7.4224-4232.2004.

Putrinš, M. *et al.* (2015) 'Phenotypic Heterogeneity Enables Uropathogenic Escherichia coli To Evade Killing by Antibiotics and Serum Complement', *Infection and Immunity* [Preprint]. Available at: https://journals.asm.org/doi/abs/10.1128/IAI.02725-14 (Accessed: 20 December 2021).

1011 Qiu, D. *et al.* (2007) 'Regulated proteolysis controls mucoid conversion in
1012 Pseudomonas aeruginosa', *Proceedings of the National Academy of Sciences*,
1013 104(19), pp. 8107–8112. doi:10.1073/pnas.0702660104.

1014 Racki, L.R. *et al.* (2017) 'Polyphosphate granule biogenesis is temporally and
1015 functionally tied to cell cycle exit during starvation in Pseudomonas aeruginosa',
1016 *Proceedings of the National Academy of Sciences*, 114(12), pp. E2440–E2449.
1017 doi:10.1073/pnas.1615575114.

1018 Samant, S. *et al.* (2008) 'Nucleotide Biosynthesis Is Critical for Growth of Bacteria in
1019 Human Blood', *PLoS Pathogens*. Edited by J.E. Galán, 4(2), p. e37.
1020 doi:10.1371/journal.ppat.0040037.

1021 Sanchez-Larrayoz, A.F. *et al.* (2017) 'Complexity of Complement Resistance Factors
1022 Expressed by Acinetobacter baumannii Needed for Survival in Human Serum', *Journal
1023 of Immunology (Baltimore, Md.: 1950)*, 199(8), pp. 2803–2814.
1024 doi:10.4049/jimmunol.1700877.

1025 Shan, Y. *et al.* (2017) 'ATP-Dependent Persister Formation in *Escherichia coli*', *mBio*.
1026 Edited by K. Bush, 8(1). doi:10.1128/mBio.02267-16.

1027 Short, F.L. *et al.* (2020) 'Genomic Profiling Reveals Distinct Routes To Complement
1028 Resistance in Klebsiella pneumoniae', *Infection and Immunity*, 88(8).
1029 doi:10.1128/IAI.00043-20.

1030 Skurnik, D. *et al.* (2013) 'A Comprehensive Analysis of In Vitro and In Vivo Genetic
1031 Fitness of Pseudomonas aeruginosa Using High-Throughput Sequencing of
1032 Transposon Libraries', *PLoS Pathogens*. Edited by B.I. Kazmierczak, 9(9), p.
1033 e1003582. doi:10.1371/journal.ppat.1003582.

1034 Trouillon, J. *et al.* (2020) 'Species-specific recruitment of transcription factors dictates
1035 toxin expression', *Nucleic Acids Res*, 48(5), pp. 2388–2400. doi:10.1093/nar/gkz1232.

1036 Ventre, I. *et al.* (2006) 'Multiple sensors control reciprocal expression of Pseudomonas
1037 aeruginosa regulatory RNA and virulence genes', *Proceedings of the National
1038 Academy of Sciences*, 103(1), pp. 171–176. doi:10.1073/pnas.0507407103.

1039 Vitkauskienė, A. *et al.* (2010) 'Pseudomonas aeruginosa bacteremia: resistance to
1040 antibiotics, risk factors, and patient mortality', *Medicina*, 46(7), p. 490.
1041 doi:10.3390/medicina46070071.

1042 Weber, B.S. *et al.* (2020) 'Genetic and Chemical Screening in Human Blood Serum
1043 Reveals Unique Antibacterial Targets and Compounds against Klebsiella
1044 pneumoniae', *Cell Reports*, 32(3), p. 107927. doi:10.1016/j.celrep.2020.107927.

1045 Winsor, G.L. *et al.* (2011) 'Pseudomonas Genome Database: improved comparative
1046 analysis and population genomics capability for Pseudomonas genomes', *Nucleic
1047 Acids Research*, 39(suppl_1), pp. D596–D600. doi:10.1093/nar/gkq869.

1048 Winsor, G.L. *et al.* (2016) 'Enhanced annotations and features for comparing
1049 thousands of Pseudomonas genomes in the Pseudomonas genome database',
1050 *Nucleic Acids Research*, 44(D1), pp. D646–D653. doi:10.1093/nar/gkv1227.

1051 Wood, L.F. and Ohman, D.E. (2012) 'Identification of genes in the sigma(2)(2) regulon
1052 of Pseudomonas aeruginosa required for cell envelope homeostasis in either the
1053 planktonic or the sessile mode of growth', *mBio*, 3(3). doi:10.1128/mBio.00094-12.

1054 Woong Park, S. *et al.* (2011) 'Evaluating the Sensitivity of Mycobacterium tuberculosis
1055 to Biotin Deprivation Using Regulated Gene Expression', *PLoS Pathogens*. Edited by
1056 M.A. Behr, 7(9), p. e1002264. doi:10.1371/journal.ppat.1002264.

1057 Wurtzel, O. *et al.* (2012) 'The Single-Nucleotide Resolution Transcriptome of
1058 Pseudomonas aeruginosa Grown in Body Temperature', *PLOS Pathogens*, 8(9), p.
1059 e1002945. doi:10.1371/journal.ppat.1002945.

1060 Yin, Y. *et al.* (2013) 'Expression of mucoid induction factor MucE is dependent upon
1061 the alternate sigma factor AlgU in Pseudomonas aeruginosa', *BMC Microbiology*,
1062 13(1), p. 232. doi:10.1186/1471-2180-13-232.

1063 Zhu, B. *et al.* (2021) 'Genome-wide identification of Streptococcus sanguinis fitness
1064 genes in human serum and discovery of potential selective drug targets', *Molecular*
1065 *Microbiology*, 115. doi:10.1111/mmi.14629.

1066

Supplementary material

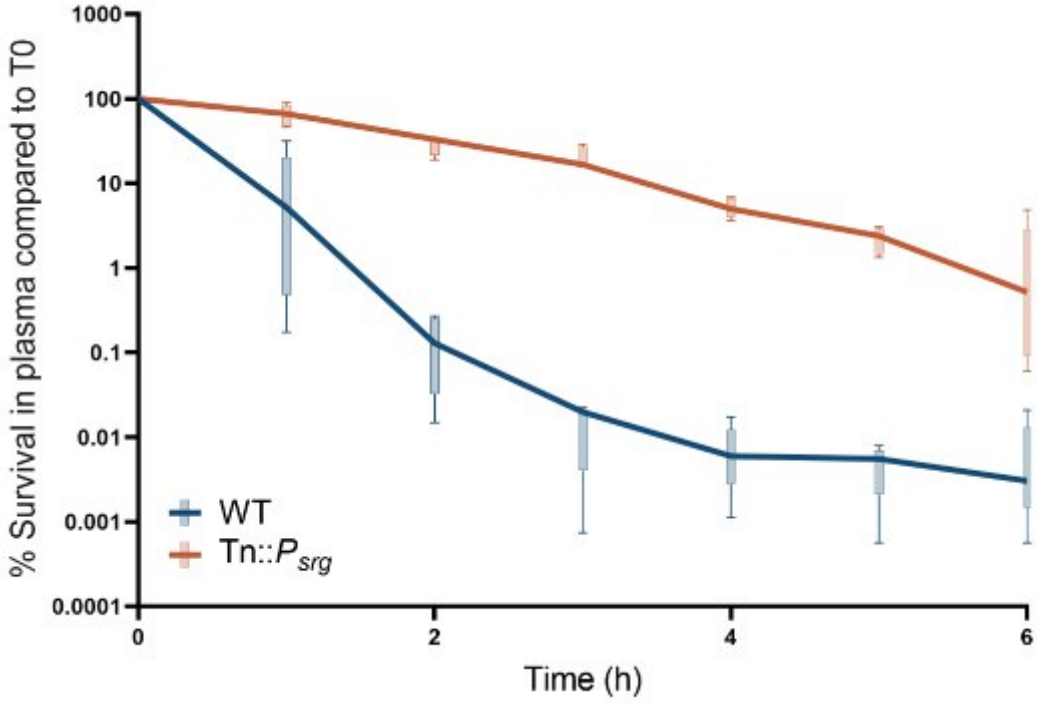

Figure S1. Overexpression of srg operon leads to a population tolerant to plasma killing. Survival kinetics of IHMA87 wild-type strain (dame data as presented in Fig. 2B) and of Tn::P_{srg} in plasma over 6h incubation measured by CFU counting (n=5).

Table 1S. Tn-seq data

Table 2S. RNA-seq differential gene expression data

Table S3. Bacterial strains and plasmids

Bacteria	Features	Reference/origin
Pseudomonas aeruginosa		
IHMA879472/AZPAE15042	Urinary isolate, plasma sensitive	IHMA[1] collection (Kos *et al.*, 2015; Pont *et al.*, 2020; Trouillon *et al.*, 2020) (Kos, Trouillon, Pont)
IHMA87Δ*bioB*	IHMA87 with *bioB* deletion	This work
IHMA87Δ*purD*	IHMA87 with *purD* deletion	This work
IHMA87Δ*algD*	IHMA87 with *algD* deletion	This work
IHMA87Δ*01134*	IHMA87 with *01134* deletion	This work
IHMA87 Tn::P_{srg}	IHMA87 with mariner transposon inserted in the promoter of *srg* operon (Gm^R)	This work
IHMA87 Tn::P_{srg} Δ*srgABC*	IHMA87 Tn::P_{srg} with *srgABC* deletion (Gm^R)	This work

IHMA87 Tn::P_{srg} Δ*srgA*	IHMA87 Tn::P_{srg} with *srgA* deletion (Gm^R)	This work
IHMA87 Tn::P_{srg} Δ*srgB*	IHMA87 Tn::P_{srg} with *srgB* deletion (Gm^R)	This work
IHMA87 Tn::P_{srg} Δ*srgC*	IHMA87 Tn::P_{srg} with *srgC* deletion (Gm^R)	This work
IHMA87 Tn::P_{srg} Δ*srgBC*	IHMA87 Tn::P_{srg} with *srgBC* deletion (Gm^R)	This work
IHMA87 Tn::P_{srg} Δ*algD*	IHMA87 Tn::P_{srg} with *algD* deletion (Gm^R)	This work
IHMA87 Tn::P_{srg} Δ*01134*	IHMA87 Tn::P_{srg} with *01134* deletion (Gm^R)	This work
IHMA87 *ladS*::Tn	IHMA87 with mariner transposon inserted in *ladS* gene (Gm^R)	This work
IHMA87 *bioA*::Tn	IHMA87 with mariner transposon inserted in *bioA* gene (Gm^R)	This work
IHMA87 *bioB*::Tn	IHMA87 with mariner transposon inserted in *bioB* gene (Gm^R)	This work
IHMA87 *mucE*::Tn	IHMA87 with mariner transposon inserted in *mucE* gene (Gm^R)	This work
IHMA87 *mucA*::Tn	IHMA87 with mariner transposon inserted in *mucA* gene (Gm^R)	This work
IHMA87 *mucD*::Tn	IHMA87 with mariner transposon inserted in *mucD* gene (Gm^R)	This work
IHMA87 *pprB*::Tn	IHMA87 with mariner transposon inserted in *pprB* gene (Gm^R)	This work
IHMA87 *mucB*::Tn	IHMA87 with mariner transposon inserted in *mucB* gene (Gm^R)	This work
Escherichia coli		
DH5α	Laboratory strain	Lab collection
TOP10	Cloning strain	Invitrogen
Plasmids		
pBTK24	Plasmid with Himar-1 mariner transposon and C9 transposase (Amp^R, Gm^R)	(Kulasekara *et al.*, 2005)
pRK600	Helper plasmid with conjugative properties (Cm^R)	(Kessler, de Lorenzo and Timmis, 1992)
pEXG2	Allelic exchange vector (Gm^R), *sacB*	(Rietsch *et al.*, 2005)
pEX18Tc	Allelic exchange vector (Tc^R), *sacB*	(Li *et al.*, 2011)
pEX100T	Allelic exchange vector (Cb^R), *sacB*	(Schweizer and Hoang, 1995)
pminiCTX-*pX2*-GFP	pminiCTX harboring the *gfp* gene under the control of a constitutive promoter (*attP* site, Tc^R)	(Thibault *et al.*, 2009)
pminiCTX-*Psrg-lacZ*	pminiCTX-*lacZ* harboring the srg promoter fused to *lacZ* reporter gene (*attP* site, Tc^R)	This work
pEXG2-mut-*bioB*	pEXG2 carrying DNA fragment for *bioB* deletion obtained by SLIC (Gm^R)	This work
pEXG2-mut-*purD*	pEXG2 carrying DNA fragment for *purD* deletion obtained by SLIC (Gm^R)	This work
pUC57-mut-*srgABC*	pUC57 carrying the synthetic DNA fragment for *srgABC* deletion in Tn::P_{srg} (Genewiz)	This work
pEX18Tc-mut-*srgABC*	pEX18Tc carrying DNA fragment for srgABC deletion in Tn::P_{srg} mutant obtained by SLIC (Tc^R)	This work
pEX18Tc-mut-01134	pEX18Tc carrying DNA fragment for IHMA87_01134 deletion obtained by SLIC (Tc^R)	This work
pEX100T-mut-*srgA*	pEX100T carrying DNA fragment for *srgA* deletion obtained by SLIC (Cb^R)	This work
pEX100T-mut-*srgB*	pEX100T carrying DNA fragment for *srgB* deletion obtained by SLIC (Cb^R)	This work

pEX100T-mut-*srgC*	pEX100T carrying DNA fragment for *srgC* deletion obtained by SLIC (Cb^R)	This work
pEX100T-mut-*srgAB*	pEX100T carrying DNA fragment for *srgAB* deletion obtained by SLIC (Cb^R)	This work
pEX100T-mut-*srgBC*	pEX100T carrying DNA fragment for *srgBC* deletion obtained by SLIC (Cb^R)	This work
pEX100T-mut-*algD*	pEX100T carrying DNA fragment for *algD* deletion obtained by SLIC (Cb^R)	This work

[1] International Health Management Association, USA

Table S4. Oligonucleotides used for PCRs

Primers	**Sequence (5'-3')**	
pEXG2-mut-*bioB*-sF1	**GGTCGACTCTAGAGGATCCCC**GTTCGGACCCCTCGAACATCG	*bioB* deletion
pEXG2-mut-*bioB*-sR1	GGTGGCGACGGCTGCGGAT	*bioB* deletion
pEXG2-mut-*bioB*-sF2	**GCGCATCCGCAGCCGTCGCCACC**CAGCTGTTCTATAACGCCGCCT	*bioB* deletion
pEXG2-mut-*bioB*-sR2	**ACCGAATTCGAGCTCGAGCCC**CTTGCCGACCAGCGCGGTGA	*bioB* deletion
F0-mut-*bioB*	GCGAGCAGCCGTTCGGCG	PCR verification for *bioB* deletion
R0-mut-*bioB*	TTGAGGCGGTCCTCCAGCA	PCR verification for *bioB* deletion
pEXG2-mut-*purD*-sF1	**GGTCGACTCTAGAGGATCCCC**CAGGAGATCCACGACCTGATCT	*purD* deletion
pEXG2-mut-*purD*-sR1	ACCGCCGCTGCCGATGATGA	*purD* deletion
pEXG2-mut-*purD*-sF2	**TACTCATCATCGGCAGCGGCGGT**GAGCGCGGCGAGTCCTGAC	*purD* deletion
pEXG2-mut-*purD*-sR2	**ACCGAATTCGAGCTCGAGCCC**TCGCGGACCAGCTGGCCGT	*purD* deletion
F0-mut-*purD*	CTGAAGATCGTCACTCGCCG	PCR verification for *purD* deletion
R0-mut-*purD*	GACTCGCCGGTGTGCTGGT	PCR verification for *purD* deletion
pEX18Tc-mut-*srgABC*-sF1	**GTCGACTCTAGAGGATCCC**CGGATCCCCGACATTCGGCTA	Transfer DNA fragment from pUC57 to pEX18Tc for *srgABC* deletion in Tn::P_{srg}
pEX18Tc-mut-*srgABC*-sR1	**CGAATTCGAGCTCGGTACCC**AAGCTTTGATCTACGTGCAAGC	
F0–mut-*srgABC*	GCCTCGCCGACCTCTACA	PCR verification for *srgA, srgB, srgC* and *srgABC* deletion
RO-Tn::P_{srg}-mut-*srgABC*	GCTTGCTGCCTTCGACCAAG	PCR verification for *srgA, srgB, srgC* and *srgABC* deletion
pEX18Tc-mut-01134-sF1	**GTCGACTCTAGAGGATCCCC**CACCTCGGTGTCCACGCTGC	IHMA87_01134 deletion
pEX18Tc-mut-01134-sR1	CGACGAGCATCGACTTGTTCAC	IHMA87_01134 deletion
pEX18Tc-mut-01134-sF2	**TGAACAAGTCGATGCTCGTC**GACAAGAACGGTCGGCTGGT	IHMA87_01134 deletion
pEX18Tc-mut-01134-sR2	**CGAATTCGAGCTCGGTACCC**ATGTTCCGCAGCCTGGTCGG	IHMA87_01134 deletion
F0-mut-01134	CTGCTGTACGTCGGCTTCCG	PCR verification for IHMA87_01134 deletion
R0-mut-01134	CTGGATGGCACCACCAACTTC	PCR verification for IHMA87_01134 deletion
pEX100T-mut-*srgA*-sF1	**ACCCTGTTATCCCTACCC**GTGATCTACG	*srgA* and *srgAB* deletion in

	TGCAAGCAGA	Tn::P_{srg}
pEX100T-mut-*srgA*-sR1	CAGGTTGCGTGAGCTGCTCA	*srgA* and *srgAB* deletion in Tn::P_{srg}
pEX100T-mut-*srgA*-sF2	**TGAGCAGCTCACGCAACCTGTGA**CCTGGACATTCTGACGAGGTA	*srgA* deletion in Tn::P_{srg}
pEX100T-mut-*srgA*-sR2	**GGATAACAGGGTAATCCC**CACCAGCGCAAGCAGCAGC	*srgA* deletion in Tn::P_{srg}
pEX100T-mut-*srgB*-sF1	**ACCCTGTTATCCCTACCC**ATGGAGGTGAACATGAGCAGC	*srgB* and *srgBC* deletion in Tn::P_{srg}
pEX100T-mut-*srgB*-sR1	AGCCAGAATCCACATGTTTC	*srgB* and *srgBC* deletion in Tn::P_{srg}
pEX100T-mut-*srgB*-sF2	**GAAACATGTGGATTCTGGCTTGA**ACGGAAGCTCGGCGCCACT	*srgB* deletion in Tn::P_{srg}
pEX100T-mut-*srgB*-sR2	**GGATAACAGGGTAATCCC**CGTGTTGACTCACGTCGGAC	*srgB* deletion in Tn::P_{srg}
pEX100T-mut-*srgC*-sF1	**ACCCTGTTATCCCTACCC**CGACGAACAGGCCTGGACAT	*srgC* deletion in Tn::P_{srg}
pEX100T-mut-*srgC*-sR1	AAGAATGACGGCGGATCGTGA	*srgC* deletion in Tn::P_{srg}
pEX100T-mut-*srgC*-sF2	**TCACGATCCGCCGTCATTCTTTGA**GATCCCAGCCTGGACTGATC	*srgC* deletion in Tn::P_{srg}
pEX100T-mut-*srgC*-sR2	**GGATAACAGGGTAATCCCC**CACTCGAAGCCGACATTCG	*srgC* deletion in Tn::P_{srg}
pEX100T-mut-*srgAB*-sF2	**TGAGCAGCTCACGCAACCTGTGA**ACGGAAGCTCGGCGCCACT	*srgAB* deletion in Tn::P_{srg}
pEX100T-mut-*srgAB*-sR2	**GGATAACAGGGTAATCCC**CGTGTTGACTCACGTCGGAC	*srgAB* deletion in Tn::P_{srg}
pEX100T-mut-*srgBC*-sF2	**GAAACATGTGGATTCTGGCTTGA**GATCCCAGCCTGGACTGATC	*srgBC* deletion in Tn::P_{srg}
pEX100T-mut-*srgBC*-sR2	**GGATAACAGGGTAATCCCC**CACTCGAAGCCGACATTCG	*srgBC* deletion in Tn::P_{srg}
pEX100T-mut-*algD*-sF1	**ACCCTGTTATCCCTACCC**CGGAAACGCCATCAAGTTGGTA	*algD* deletion
pEX100T-mut-*algD*-sR1	GCCAGCACATACCGCACCGA	*algD* deletion
pEX100T-mut-*algD*-sF2	**TCGGTGCGGTATGTGCTGGC**CAGGCCGAGGGCATCTGCT	*algD* deletion
pEX100T-mut-*algD*-sR2	**GGATAACAGGGTAATCCC**GCTGTCGATGGCTTCGCGGA	*algD* deletion
F0-mut-*algD*	CTCGTGGCGAATAGGCCTAC	PCR verification for *algD* deletion
R0-mut-*algD*	GCGAAGCGCAGCTTGTGCC	PCR verification for *algD* deletion
Primers for Tn-seq		
Short adpator	TACCACGACCA-NH2	
Long adaptor	GTGACTGGAGTTCAGACGTGTGCTCTTCCGATCTGGTCGTGGTAT	
PCR1 Tn-specific	CACAGGAAACAGGACTCTAGAGG	
PCR2 adaptor complementary	GTGACTGGAGTTCAGACGTGTG	
P5+ Illumina	AATGATACGGCGACCACCGAGATCTACACTCTTTCCCTACACGACGCTCTTCCGATCTCTAGAGACCGGGGACTTATCAGC	
P7-index	CAAGCAGAAGACGGCATACGAGAT**CGTGAT**	

Supplementary references

Kessler, B., de Lorenzo, V. and Timmis, K.N. (1992) 'A general system to integrate *lacZ* fusions into the chromosomes of gram-negative eubacteria: regulation of thePm promoter of theTOL plasmid studied with all controlling elements in monocopy', *Molecular and General Genetics MGG*, 233(1–2), pp. 293–301. doi:10.1007/BF00587591.

Kos, V.N. *et al.* (2015) 'The resistome of Pseudomonas aeruginosa in relationship to phenotypic susceptibility', *Antimicrob Agents Chemother*, 59(1), pp. 427–36. doi:10.1128/AAC.03954-14.

Kulasekara, H.D. *et al.* (2005) 'A novel two-component system controls the expression of Pseudomonas aeruginosa fimbrial cup genes', *Molecular Microbiology*, 55(2), pp. 368–380. doi:10.1111/j.1365-2958.2004.04402.x.

Li, S. *et al.* (2011) 'Physiological role of the novel salicylaldehyde dehydrogenase NahV in mineralization of naphthalene by Pseudomonas putida ND6', *Microbiological Research*, 166(8), pp. 643–653. doi:10.1016/j.micres.2011.01.003.

Pont, S. *et al.* (2020) 'Bacterial behavior in human blood reveals complement evaders with some persister-like features', *PLoS Pathog*, 16(12), p. e1008893. doi:10.1371/journal.ppat.1008893.

Rietsch, A. *et al.* (2005) 'ExsE, a secreted regulator of type III secretion genes in Pseudomonas aeruginosa', *Proceedings of the National Academy of Sciences*, 102(22), pp. 8006–8011. doi:10.1073/pnas.0503005102.

Schweizer, H.P. and Hoang, T.T. (1995) 'An improved system for gene replacement and xylE fusion analysis in Pseudomonas aeruginosa', *Gene*, 158(1), pp. 15–22. doi:10.1016/0378-1119(95)00055-B.

Thibault, J. *et al.* (2009) 'Anti-activator ExsD forms a 1:1 complex with ExsA to inhibit transcription of type III secretion operons', *The Journal of Biological Chemistry*, 284(23), pp. 15762–15770. doi:10.1074/jbc.M109.003533.

Trouillon, J. *et al.* (2020) 'Species-specific recruitment of transcription factors dictates toxin expression', *Nucleic Acids Res*, 48(5), pp. 2388–2400. doi:10.1093/nar/gkz1232.